이학박사학위논문

# 중심체 단백질인 CPAP와 CP110의 기능에 관한 연구

**Studies on the Function of Centrosomal Proteins, CPAP and CP110**

2015년 2월

서울대학교 대학원
생명과학부
이 미 선

# 중심체 단백질인 CPAP와 CP110의 기능에 관한 연구

**Studies on the Function of Centrosomal Proteins, CPAP and CP110**

지도교수 이 건 수

이 논문을 이학박사 학위논문으로 제출함

2015년 2월

서울대학교 대학원

생명과학부

이 미 선

이미선의 이학박사 학위논문을 인준함

2015년 2월

위 원 장 _____(인)

부위원장 _____(인)

위 원 _____(인)

위 원 _____(인)

위 원 _____(인)

# Studies on the Function of Centrosomal Proteins, CPAP and CP110

*A dissertation submitted in partial*

*fulfillment of the requirement*

*for the degree of*

**DOCTOR OF PHILOSOPHY**

**to the Faculty of**

**School of Biological Sciences**

**at**

**Seoul National University**

**by**

**Miseon Lee**

**Feb, 2015**

**Date Approved:**

_____ _____

_____

_____

_____

_____

# Abstract

A centrosome consists of a pair of centrioles embedded in pericentriolar materials (PCM). Like chromosomes, centrioles duplicate and segregate into the daughter cells. Centriole duplication is strictly regulated to occur once per cell cycle. Abnormalities in the number of centrioles lead to chromosome instability and tumor formation. During mitosis, centrosomes prepare to become spindle poles and undergo maturation which PCM is accumulated at the centrosome to possess a strong microtubule organizing activity. If the centrosomes fail to become mature, the chromosomes do not properly segregate to daughter cells. Therefore, it is essential to elucidate precise mechanisms of centrosome duplication and maturation during the cell cycle. Here, I investigated the functions of two centrosomal proteins, CPAP (Centrosomal protein 4.1-associated protein) and CP110 (Centrosomal protein of 110kDa) to study centrosome maturation and duplication.

In Chapter 1, I investigated biological roles of CPAP in centrosome maturation. It is known that CPAP functions in centriole assembly and elongation. I found that CPAP is also critical for centrosome maturation during mitosis. The CPAP function in centrosome maturation is independent of centriole duplication. Depletion of CPAP eventually resulted in asymmetric spindle pole formation during mitosis. Asymmetric spindle pole indicates that the mitotic spindle pole have uneven amount of PCM.

In chapter 2, I investigated biological roles of CP110 in centriole duplication. PLK4 is a critical kinase in centriole assembly. However, direct substrates of PLK4 remain elusive. I demonstrated that CP110 is phosphorylated by PLK4 in vivo. This

phosphorylation is prerequisite of the centriole assembly. The phosphorylated CP110 is recruited at the proximal end of the daughter centrioles at an early stage of centriole assembly. Based on these results, I propose that phosphorylation of CP110 by PLK4 is a critical step for stabilization of the recruited centriole components.

***Keywords:*** Centrosome, CPAP, Pericentriolar material (PCM), centriole maturation, CP110, PLK4, centriole duplication

***Student Number:*** 2010-30100

# Contents

# List of Figures

# Background

# 1. The origin and evolution of the centrosome

Centriole/basal bodies (CBBs) are cylindrical organelles composed by microtubules. These organelles form centrosome, cilia, and flagella. Because CBBs, cilia, and flagella are present in all major eukaryotic groups, they are regarded as ancestral structures.

## 1.1 Molecular mechanism of centriole/basal bodies evolution

In the past decade, many centrosome components were identified, and function of these proteins were studied in model organisms. In particular, studies in *Caenorhabditis elegans* and *Drosophila* revealed that many structural components and regulators of centriole duplication are conserved across ciliated eukaryotes, such as Sas-6, Sas-4/CPAP, and Bld10/CEP135 (Nigg and Stearns, 2011). Despite the conservation of these components, new proteins appear to have been added throughout evolution (Carvalho-Santos et al., 2010; Hodges et al., 2010). For instance, CP110 and CEP97 cooperatively function in cilia assembly. These two proteins are only present to the metazoans (Carvalho-Santos et al., 2010; Hodges et al., 2010). It is thought that these proteins might have been added to cilium assembly pathway.

# 2. The centrosome

The centrosome is an organizer of the microtubule cytoskeleton. Centrosomes associate with the nuclear envelope and are usually locates at the center of the cells.

## 2.1. Function of the centrosome

The centrosome functions in cell polarity and cell division, and development

of most animals. In interphase cells, astral microtubules (MT) that emanate from the centrosome determine cell shape, polarity, and motility (Desai and Mitchison, 1997) (Keating and Borisy, 1999). In most epithelial cells, centrioles move to apical surface of the cells (Dylewski and Keenan, 1984). Movement of centriole is accompanied by formation of apical-basal MTs and loss of radial MTs (Rieder et al., 2001). This positioning of centrosome in cells determines geometry.

In mitosis, the centrosome forms the bipolar spindle. Bipolar spindle is critical for faithful segregation of chromosomes. In dividing cells, centrosome based spindle axis determines cell fate. For example, in neuroblasts, symmetric division makes two daughter neuroblasts. So symmetric division in neuroblasts expand the progenitor pool, whereas, asymmetric division with perpendicular spindle axis generate one neuroblast and differenciating cell (Yamashita and Fuller, 2008). The centriole functions as basal bodies of the cilia and flagella. Cilia and flagella sense extracellular signals such as moving fluid and cell motility.

### 2.2. Structure of the centrosome

The centrosome is composed of two centrioles and pericentriolar materials (PCM) surrounding two centrioles.

#### 2.2.1. Centrioles

Centriole is composed of nine microtubules (MT). There are structural variations in different species. *C. elegans* and *Drosophilla* embryo have singlet and doublet microtubules, respectively. In human, nine triplet microtubules are arranged into a cylinder shape. In vertebrate and most cell types, the length of cylinder is approximately 500nm and diameter is approximately 250 nm.

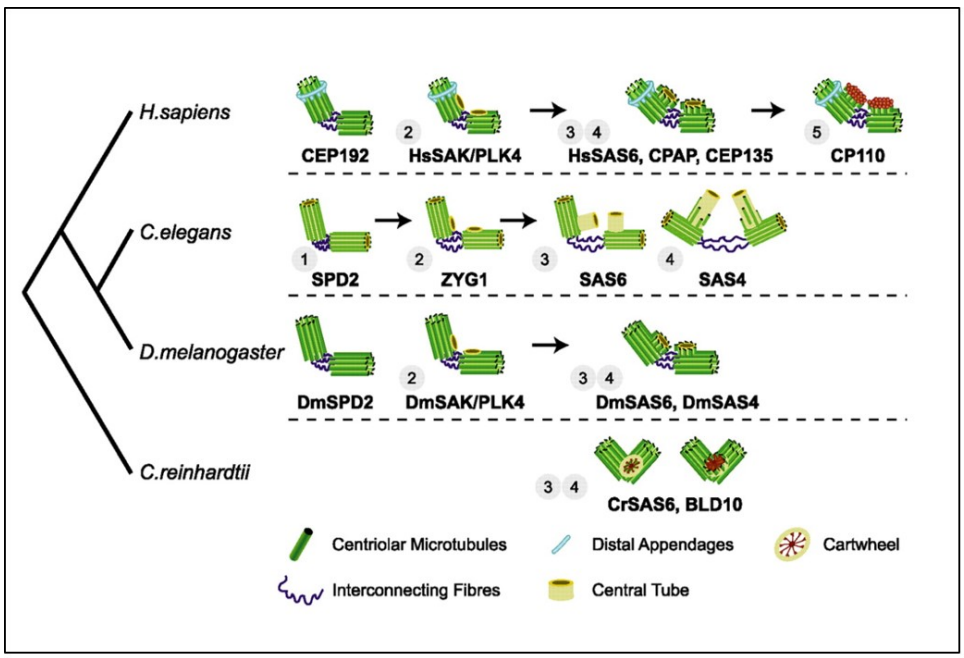


(Carvalho S et al., *J Cell Biol* **123**:1414-1426, 2010)

**Figure 1. Evolutionally conserved components of centriole duplication.** Despite of a great structural diversity, they share core component of centriole assembly. SAS-6, SAS4/CPAP and BLD10/CEP135 three components correlates with the occurrence of centriole and basal body.

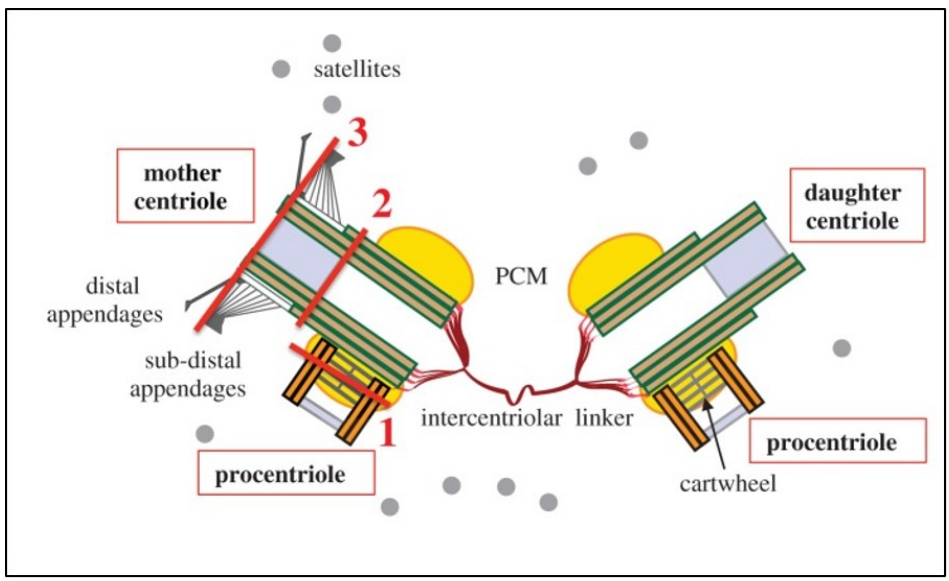


(Bornens M and Gonczy P, *Philos Trans R Soc Lon Biol Sci* **369:**1650, 2014)

**Figure 2. The structure of the centrosome.** The figure represents a pair of centrosome in human cells during S phase. The centrosome is composed of two centrioles and pericentriolar material (PCM). The microtubules that make up the wall of centrioles. The mother centrioles are approximately 450 nm long and approximately 250 nm in diameter. Only the mother centriole has appendage structure at distal tip of the centriole. Procentrioles have cartwheel structure at proximal part of the centrioles

A triplet microtubule contains a complete microtubule, which is called A-tubule, and additional two partial microtubules are B-, C- tubules. Centriole has polarity with microtubule minus ends at proximal end of the centriole. In this proximal centrioles with microtubule minus end, new centriole is assembled. New assembled centriole is orthogonally arranged next to previous centrioles. New centrioles are assembled using the cartwheel, which is a subcentriolar structure containing nine radial and functions as central hub.

Among the two orthogonally arranged centrioles, one is older than the other. The older one is mother centriole, which was formed in previous duplicating cycle, and the younger other is daughter centriole, which is newly formed in this duplication cycle. Two centrioles are structurally different. The older mother centriole has distal and subdistal appendages at its distal part of centriole, newly formed daughter centriole lacks. This distal and subdistal appendages are markers of maturation (Paintrand et al., 1992; Vorobjev and Chentsov Yu, 1982), since these structures are part of old centrioles. Several components such as CEP164, CCDC123/CEP89/CEP123, CCDC41 are found in this distal appendages (Jana et al., 2014).

The distal appendages are fibrous radiating structure, which function in primary cilia formation. This structure is required for cilia assembly. Subdistal appendages locate proximal to the distal appendages and attach laterally to microtubule scaffold. Ninein, centriolin, CEP170 are subdistal appendage proteins (Jana et al., 2014). The subdistal appendage functions in microtubule anchoring (Kodani et al., 2013). Only the pre-existing old centriole acquires this structure at G2

and M phase and functions in anchoring to microtubules.

### 2.2.2. Filamentous structure

Upon duplication, two centrioles are connected to each other via a filamentous structure (Bornens et al., 1987). The filamentous C-Nap1 and Rootletin interact and localized to this structure (He et al., 2013). This filamentous structure is dissociated at G2 phase through C-Nap1 dissociation upon phosphorylation by Nek2. Then, two duplicated centrioles move apart (Fry et al., 1998).

### 2.2.3. Pericentriolar materials (PCM)

Centrioles organize the PCM on the outside the microtubules. According to electron previous microscopy results, the PCM appeared as amorphous mass surrounding centrioles (Robbins et al., 1968). Large scale RNAi and localization screen revealed many PCM proteins (Leidel and Gonczy, 2003). Previous conventional microscopy could not give the precise structural information about PCM. However, recent advances in light microscopy, such as three dimensional structured illumination microscopy (3D-SIM) and stochastic optical reconstruction microscopy (STROM) allowed to observe PCM structure (Fu and Glover, 2012; Mennella et al., 2012; Sonnen et al., 2012). Through these advances, researchers were able to locate important proteins nearby centriole by measuring the distance from the outer centriole (Mennella et al., 2012; Sonnen et al., 2012). Also, they found that interphase PCM are assembled in concentric toroid structure forming discrete diameter shape.

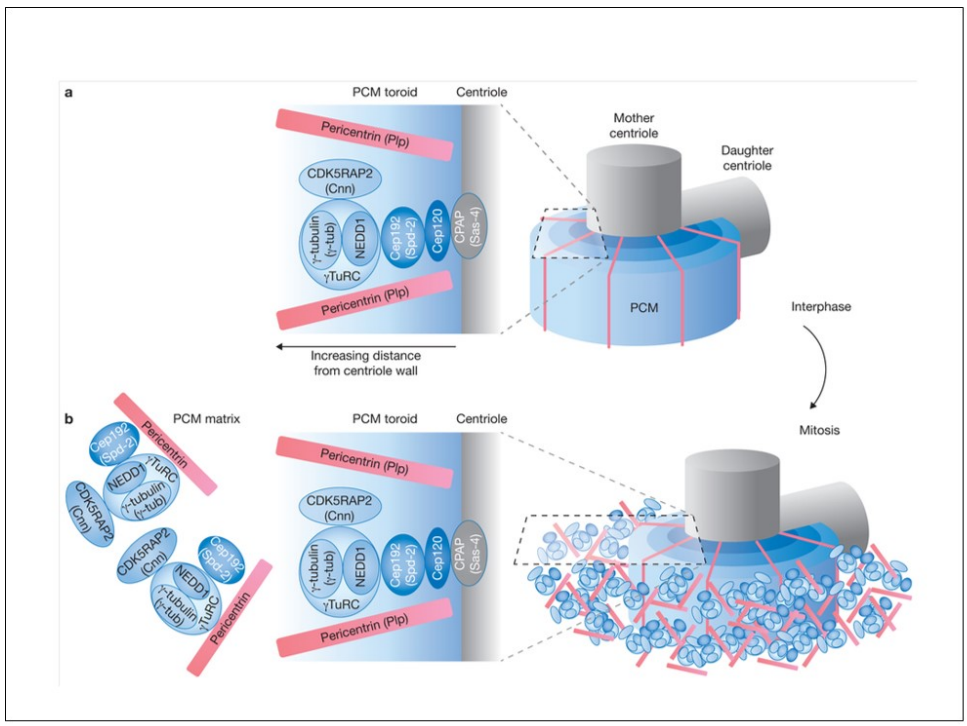


(Luders J, *Nature Cell Biol* **14**:1126-1128, 2012)

**Figure 3. The centrosome and pericentriolar materials (PCM).** The centrosome embedded in a matrix of proteins known as the pericentriolar material (PCM). The pericentriolar material is composed of multiple proteins. During interphase, PCM proteins are organized in toroids structure around mother centrioles. Gamma-tubulin is one of the major PCM proteins and localizes at outer layer of the PCM. Gamma-tubulin functions in microtubule nucleation. In G2 and M phase, this PCM is expanded preparing strong spindle pole.

# 3. Centrosome duplication

## 3.1. Initiation

In centriole duplication cycle, the first step is the formation of a procentriole next to the mother centriole. Centriole assembly is followed by hierarchial protein recruitment, but the precise mechanism is poorly understood in mammals.

PLk4 is thought to be a critical kinase that regulates the onset of centriole assembly. PLK4, a polo-like kinase 4, is required for centriole assembly (Kim et al., 2013). In *C.elegans*, ZYG-1, a functional orthologue of PLK4 recruits sas6, indicating that this is an evolutionarily conserved mechanism (Lettman et al., 2013). Some proteins have been reported as a substrate of PLK4, such as GCP6 (Bahtz et al., 2012; Chang et al., 2010; Hatch et al., 2010; Puklowski et al., 2011). However, there is no critical link to explain PLK4 kinase activity and centriole assembly. Recently, one group showed that STIL interacts with and is phosphorylated by PLK4 and functions in sas6 recruitment (Ohta et al., 2014). Also, CEP152 and CEP192 interact with PLK4 and cooperatively function in PLK4's recruitment to the centriole (Kim et al., 2013).

## 3.2. Cartwheel assembly

Once the centriole assembly site is determined at mother centrioles, cartwheel structure is assembled at this site (Cottee et al., 2011). This is the first visible sign of procentriole formation. Sas6 is a key cartwheel assembly component. It forms oligomers and ring-like organization (Hirono, 2014; van Breugel et al., 2014). Bld10/CEP135 functions together to establish and stabilize the cartwheel ninefold

symmetry (Roque et al., 2012).

Interestingly, in matured centrioles in mammals, the cartwheel is lost (Gonczy, 2012; Keller et al., 2014), indicating that this structure is required for initiation of procentriole formation but not for maintenance. Since cartwheel is localized to proximal part of centrioles and linked to the proximal end of the mother centrioles (Guichard et al., 2010), it is likely to be the potential bridge that connects procentriole to mother centriole.

### 3.3. Centriole microtubule recruitment

Next, how are microtubules recruited to cartwheel to form the microtubule triplets? It is reported that gamma-tubulin localizes to the core centrioles, in addition to pericentriolar materials (Moudjou et al., 1996). Gamma-tubulin, in association with the cartwheel, enforces growth of A-tubule. After nucleation of A-tubules, B- and C-tubules assembled (Guichard et al., 2010). There are two proteins CPAP and Centrobin, which interact with tubulin (Gudi et al., 2011; Tang et al., 2009). CPAP is accumulated in procentriole. In *C.elegans* SAS4, orthologue of CPAP, functions in tubulin recruitment. Centrobin is a daughter centriole marker, and the disruption of centrobin-tubulin interaction results in destabilizing of pre-existing centrioles (Gudi et al., 2011).

### 3.4. Centriole elongation

Centriole elongation occurs after centriole formation during G2 and M phase. Many reports showed that regulation of centriole length is result of antagonistic functions of CPAP and CP110 (Comartin et al., 2013; Lin et al., 2013; Schmidt et al., 2009). Overexpression of CPAP induces longer centrioles, indicating that CPAP

positively regulate centriole elongation (Kohlmaier et al., 2009). Phosphorylation of CPAP is critical for stabilizing centriolar microtubules and elongation. CP110 is capping protein which localize at distal part of centriole. This cap should be removed for the formation of cilia (Tsang et al., 2008).

# 4. Centriole number control

## 4.1. Control of protein level

Centrosome duplication is tightly regulated process, which occurs only once per cell cycle. Abnormalities in centriole number and structure are associated with genomic instability, and centriole amplification is a hallmark of cancer. Although multiple centrioles can form bipolar spindles through clustering, they increase the incidence of merotelic attachments and could induce genomic instability.

PLK4 has a key role in controlling centriole duplication. Overexpression of PLK4 results in centrosome amplification (Bettencourt-Dias et al., 2005; Habedanck et al., 2005; Kleylein-Sohn et al., 2007). It is well known that the amount of PLK4 is critical; therefore regulation of PLK4 level has been well studied (Brownlee et al., 2011; Rogers et al., 2009). It is reported that PLK4 forms homodimer, autophosphorylates at multiple sites, and is degraded by $SCF^{\beta TrCP}$ (Holland et al., 2012; Holland et al., 2010). Through this regulation, the level of PLK4 is strictly regulated during the cell cycle, and the regulation of PLK4 may control the centriole assembly, by phosphorylating its substrates.

In addition to PLK4, other centriole components also regulate centriole number. For example, overexpression of STIL and Sas6 (Arquint and Nigg, 2014; Kitagawa et al., 2011; Leidel and Gonczy, 2003) forms extra centrioles. Both STIL

and SAS6 are degraded during mitosis through anaphase promoting complex (APC/C) dependent degradation pathway (Arquint and Nigg, 2014; Kitagawa et al., 2011). Similar to PLK4, sas6 is also regulated by FBXW5 dependent degradation during G2 phase (Puklowski et al., 2011), and this degradation is critical for duplication control.

### 4.2. Centrosome-intrinsic block

It is reported that centrosome-intrinsic mechanism blocks centriole reduplication during S and G2 phase (Nigg, 2007). According to this licensing model, the engagement of duplicated centrioles blocks re-duplication until the end of mitosis. At the end of mitosis, centrioles disengage, licensing duplication. In vertebrates, the activities of PLK1 and separase are required for disengagement (Lee and Rhee, 2012; Matsuo et al., 2012; Tsou et al., 2009)

### 4.3. CDK2 in centriole duplication

CDK2 kinase is also involved in centriole duplication. CDK2 is active during G1/S transition. It is reported that CDK2 is required for centriole overduplication in somatic cells (Duensing et al., 2006; Meraldi et al., 1999) and normal duplication in *Xenopus* eggs (Hinchcliffe et al., 1999). However, CDK2 activity appears dispensable for normal duplication in cycling cells (Meraldi et al., 1999). However, CDK2 activity is required for PLK4 induced overexpression. This suggests that there is redundant mechanism related to CDK2 in centriole assembly.

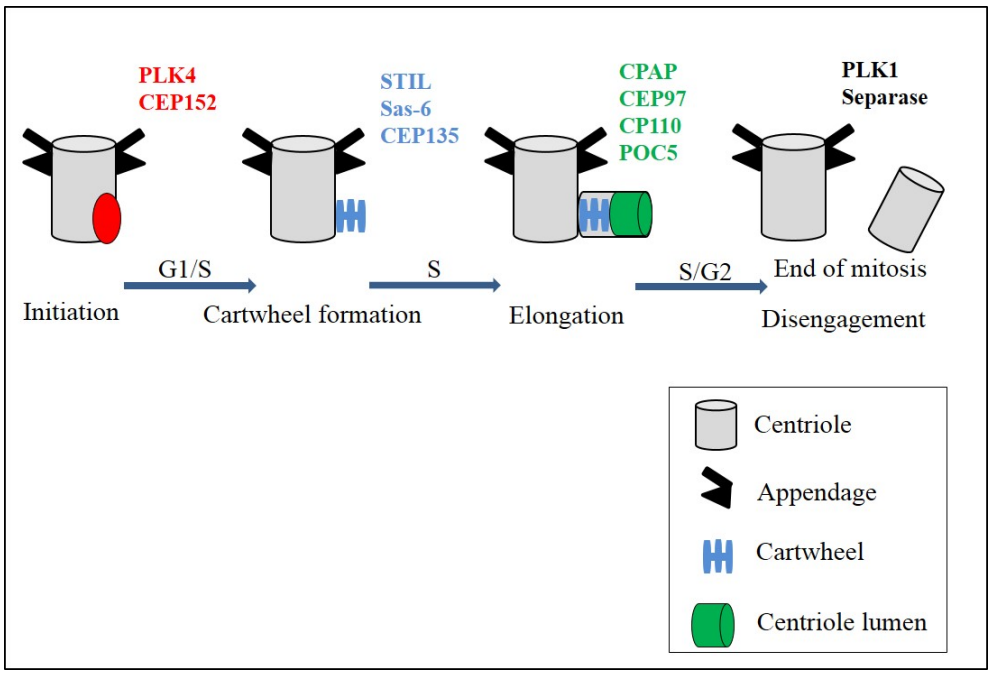


**Figure 4. Procentriole assembly.** At G1/S transition**,** PLK4 Kinase and CEP152 initiates the cartwheel formation. Mother centriole acquires a single focus of PLK4. At this site, Sas-6, Cep135, STIL are recruited. They forms cartwheel structure at early S phase. During S and G2 phase, procentrioles are elongated. CPAP promotes centriolar microtubule elongation around the cartwheel. CP110 and CEP97 localize at distal part of the centriole and stabilize it. End of mitosis, centrioles are disengaged PLK1- and separase-dependent manner. Cartwheel is lost from the procentriole after disengagement.

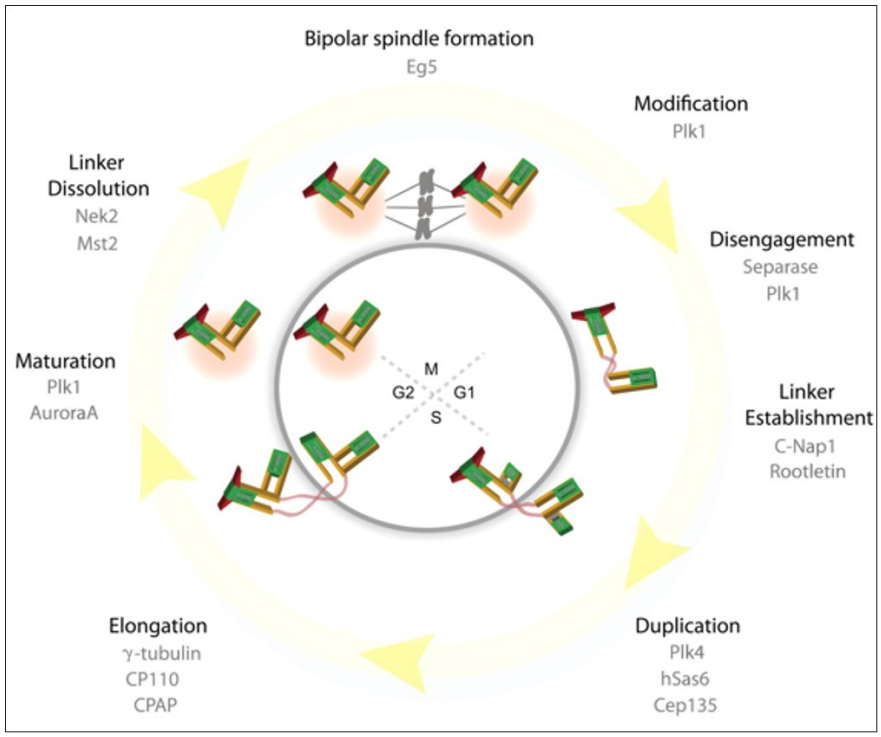


(Mardin B R, and Schiebel E *J Cell Biol* **197:**11-18, 2012)

**Figure 5. The centrosome cycle.** The centrosome cycle initiates in G1/S transition. At G1 phase, mother and daughter centrioles are disengaged. At G1/S transition, procentrioles are assembled next to pre-existing centrioles. In this stage, two mother centrioles (pre-existing) are in different age. One is the old mother centriole and the other is the young mother centriole. Only the old mother centriole has appendage structure that is acquired at previous cell cycle. During S and G2 phase, procentrioles are elongated. At G2 phase, young mother centriole acquires appendage structure. This is the centriole maturation. Together with centriole maturation, PCM size also increased preparing mitosis. At mitosis, two centrosomes separate and function in mitotic spindle pole. The end of mitosis, two centrosomes segregate to each daughter cells.

# 5. Health and disease

## 5.1. Centrosome number and cancer

Centrosome amplification is a hallmark of cancer. Centrosomal abnormalities have been reported in many solid tumors, such as colon, breast, ovarian cancer (Hsu et al., 2005; Lingle et al., 1998), in addition to myeloma, acute and chronic leukemia. Some reports suggest that abnormality of centrioles causes tumor initiation; however, this hypothesis remains controversial. There are two types of centrosome abnormalities.

### 5.1.1. Structural defect

Structural defects reflect deregulation such as phosphorylation of centrosomal components (Nigg, 2006). There are two structural defects; defects in centriole structure and in the amount of PCM.

### 5.1.2. Numerical defect

Numerical defects show excessive numbers of centrioles. The cause of amplified centrioles could be either division failure or overduplication. Centriole overduplication may be cause by defects in cell cycle control or duplication number control.

Deregulation of ubiquitin regulators may result in changes in the stability of centriole proteins. For instance, $SCF^{\beta TrCP}$ downregulation leads to the stabilization of CP110 level. Both cases result in centriole amplification**.**

## 4.2. Centrosome and microcephaly

Autosomal primary microcephaly (MCPH) is a neurodevelopmental disorder caused by mutations in several genes. MCPH patients have small brain size, with

mental retardation (Kumar et al., 2009). Of the nine genes implicated in MCPH, CPAP CEP152, CEP135, STIL and CDK5RAP2 genes encode core centrosomal components, and ASPM and WDR62 are related to mitotic spindle poles. Cells with defects in centriole number take longer time to make a bipolar spindle (Kwon et al., 2008; Novorol et al., 2013).

In brain development, balance between pools of progenitors and differentiating cells is important, and determination of cell fate depends on cell division axis. In early development, neuronal progenitors have perpendicular axis to apical surface and make two progenitors. In this division, progenitor pool is highly increased. Defect in genes involved in MCPH results in abnormal spindle orientation (Kitagawa et al., 2011). This uncontrolled orientation may cause decrease of progenitor pools.

### 4.3. Ciliopathy

Ciliopathy is genetic disorders caused by defects in ciliary function or structure. Ciliopathy affects most organs, such as kidney, eye, liver and brain. In ciliopathy, impairment in cell signaling is considered a key factor (Chavali et al., 2014).

# Chapter 1

# Asymmetric spindle pole formation in CPAP-depleted mitotic cells

# Abstract

It is known that SAS-4 and its human homologue, CPAP, are essential for centriole assembly and centriole elongation. Here, I report that CPAP is also involved in spindle pole formation during mitosis. Centriole, especially mother centriole has a capacity to recruit pericentriolar materials (PCM). In knockdown-rescue experiment, I observed that the amount of PCM was asymmetrically distributed between the mitotic spindle poles of CPAP-depleted cells. The mother centriole lengths in CPAP-depleted cells were identical to those of control cells, indicating that the spindle pole asymmetry in CPAP-depleted cells is not due to the shortened size of mother centrioles between the spindle pole pair. Rather, centriole maturation was inhibited in CPAP-depleted cells, as evidenced by the absence of distal and subdistal appendage proteins. My results predict that neural stem cells in *CPAP* mutant individuals might have defects in spindle orientation, which causes a reduction in the stem cell population and subsequent reduction of the differentiated cell population.

***Keywords:*** CPAP, Centriole maturation, spindle pole, mitosis

# Introduction

The centrosome is a major microtubule-organizing center that consists of a pair of centrioles surrounded by pericentriolar materials (PCM). Centrioles duplicate and segregate in tight association with the cell cycle. Procentrioles begin to form next to mother centrioles at the G1/S phase. The procentrioles are elongated, and they eventually disengage from the mother centriole at the end of mitosis. Centriole disengagement is considered important for licensing a new round of centriole duplication (Tsou and Stearns, 2006). The disengaged centriole becomes a mother centriole when a new procentriole is formed next to it. However, this young mother centriole is still structurally immature. For example, the young mother centriole lacks distal and subdistal appendages until the cell undergoes mitosis (Loncarek and Khodjakov, 2009). Therefore, it takes one and a half cell cycles for a procentriole to become a fully matured mother centriole.

Genetic analysis in *Caenorhabditis elegans* identified a number of centriolar proteins that are involved in centriole assembly, such as ZYG-1, a protein kinase, and SAS-4, SAS-5, SAS-6 and SPD-2, which contain coiled-coil domains (Leidel and Gonczy, 2003; O'Connell et al., 2001). During centriole biogenesis, these proteins are sequentially recruited to centrioles (Pelletier et al., 2006). ZYG-1 recruits SAS-5 and SAS-6, which are required to SAS-4 incorporation (Dammermann et al., 2008; Pelletier et al., 2006). It is proposed that the centriole duplication mechanism is evolutionally conserved from *C. elegans* to human (Kleylein-Sohn et al., 2007). CPAP, the human homologue of SAS-4, is essential for centriole formation in human cells

(Chang et al., 2010; Kohlmaier et al., 2009; Schmidt et al., 2009; Tang et al., 2009). During the G2 and M phase, the centrosomes are matured, accumulating γ-tubulin and PCM proteins (Palazzo et al., 2000). This process is called centrosome maturation. The matured mitotic centrosome functions as mitotic spindle poles.

Primary microcephaly is a rare, recessive genetic disease in which the prenatal brain growth is significantly reduced while the brain structure is left intact (Thornton and Woods, 2009). It was proposed that the reduction in neuronal cell number during development is the causal event of microcephaly (Bond et al., 2005). Neocortex stem cells are originally generated by symmetrical division of the neural tube epithelium at the ventricular zone. Once neurogenesis begins, the stem cells initiate asymmetric division to generate differentiated neural cells. Therefore, it is important to switch from symmetric to asymmetric cell division at the appropriate time. Spindle pole orientation in stem cell division is a critical factor for cell fate determination and eventually for tissue organization. The spindle pole position in neural progenitor cells is determined by the spindle pole itself as well as by cortical polarity cues (Gillies and Cabernard, 2011). In fact, mutations in genes coding for centrosomal proteins were detected in a number of primary microcephaly patients (Bond et al., 2005).

*CPAP* is one of the causal genes implicated in primary microcephaly (Bond et al., 2005). However, it is not understood how the neural cell number is reduced in individuals with *CPAP* mutations. In this study, I revealed that CPAP-depletion results in the asymmetry of spindle pole activity, which probably results in the premature initiation of asymmetric cell division.

# Materials and methods

## Transfection and RNA interference

*siCPAP* (GGA CUG ACC UUG AAG AGA ATT), *siCTL* (scrambled sequence for control) (GCA AUC GAA GCU CGG CUA CTT), *siCenexin1* (AGA CUA AUG GAG CAA CAA G) were used for RNAi experiments. The siRNAs were transfected into HeLa cells using RNAi MAX reagents (Invitrogen). Plasmids were transfected with FuGENE HD (Roche). For rescue experiment, siRNAs and DNAs were sequentially transfected

## Antibodies

CPAP antibody was raised against C-terminus of CPAP and affinity purified with GST-CPAP$^{979\text{-}1338}$(Chang et al., 2010), CEP135 (Kim et al., 2008), and CP110 antibodies were generated and affinity purified against GST-CEP135$^{295\text{-}1141}$, CP110$^{1\text{-}334}$, respectively. Ninein antibody was raised against GST-Ninein$^{381\text{-}689}$. Centrin-2 rabbit polyclonal antibodies were also raised against GST-Centrin-2$^{1\text{-}172}$. Antibodies against γ-tubulin (C-20, Santa Cruz Biotechnology, Inc.), cyclin B1 (GNS1, Santa Cruz Biotechnology), Acetylated-tubulin (T6199, Sigma), Flag (F3165, Sigma), α-tubulin (ab18251, Abcam), Sas-6 (91.390.21, Santa Cruz Biotechnology) antibodies were purchased. hCenexin1 (Soung et al., 2006) antibody was given from Kyung S. Lee

## Cell culture and cell cycle synchronization

HeLa cells were grown at 37°C and 5% $CO_2$ in high glucose DMEM supplemented with 10% fetal bovine serum. To synchronize cells in G2 phase,

HeLa cells were arrested at G1/S phase by double-thymidine block and released for 8 h and then cells were fixed. In the rescue experiments, mitotic cells were synchronized at S phase by thymidine block and release followed by MG132 treatment for 1 h.

**Immunoblot analysis**

Cultured HeLa cells were lysed in the sample buffer (50 mM Tris-HCl, pH 6.8, 100 mM dithiothreitol, 2% SDS, 0.1% bromophenol blue, 10% glycerol). Samples were loaded in 8% and 4% polyacrylamide gels and then transferred into nitrocellulose membranes. The membranes were blocked in 5% skim milk in TBST (20 mM Tris, 150 mM NaCl, 0.3% Triton X-100) for 30 min, incubated with antibodies for overnight at 4℃. After washing three times with TBST for 7 min, the membranes were incubated with mouse and rabbit secondary antibodies (1:10,000) for 40 min. After the membranes were washed three times with TBST for 5 min, the peroxidase activity was detected using ECL solutions.

**Immunofluorescence and Microscopy**

For indirect immunocytochemistry, HeLa cells were grown on 12-mm coverslips and fixed with cold 100% methanol for 10 min. The cells were then permeabilized and blocked with 3% BSA in 0.5% PBST for 15 min. Primary antibodies were diluted in 3% BSA in 0.5% PBST, incubated at room temperature for 1 or 2 h and coverslips were washed three times in 0.1% PBST. Secondary antibodies were diluted in 3% BSA in 0.5% PBST, incubated for 30 min at room temperature and washed again three times in 0.1% PBST. For DNA staining, DAPI solution was used at the final step for 4 min. The coverslips were mounted on slides and observed with a

fluorescence microscope (Olympus IX51) equipped with a CCD camera (Qicam fast 1394, Qimaging). Images were processed using ImagePro 5.0 (Media Cybernetics, Inc.) and statistic analyzed with Sigma Plot (Systat Software, Inc.).

To measure the length of centrioles, we used a super-resolution structured illumination microscopy (SIM; Nikon N-SIM) equipped with a CFI Apo TIRF 100× oil objective lens (NA1.49) and iXon DU-897 EMCCD camera. The images were taken as Z-stack with distance between planes of 0.1 μm. The center of the signal was determined by intensity profile in NIS-Elements software. The antibodies were conjugated with Alexa Fluor 555 dyes (Molecular Probes).

# Results

## Centriole reduction in CPAP-depleted mitotic cells

CPAP is an essential centrosome component for centriole assembly since CPAP depletion results in defects in centriole duplication (Chang et al., 2010; Tang et al., 2009). To begin my study, I decided to observe defects of centriole duplication in CPAP-depleted mitotic cells. I immunostained the mitotic cells with a centrin-2 antibody to count the number of centrioles at each mitotic spindle pole. The results showed that the number of centrioles in CPAP-depleted cells decreased (Figure 6). The phenotype became severe in correlation to the knockdown period (Figure 6). It is interesting that diverse patterns of centriole numbers were observed even if the centrosomal CPAP is effectively depleted.

## Asymmetric spindle poles in CPAP-depleted cells

In CPAP-depleted mitotic cells, I observed asymmetric spindle pole compared to control cells. Asymmetric spindle poles are composed of two poles with different amount of PCM. Spindle poles were determined as asymmetric when the intensity of one pole was at least 1.5 fold higher than the other pole within one cell. To confirm this asymmetric spindle pole phenotype is caused by CPAP-knockdown, I performed knockdown and rescue experiments with ectopic Flag-CPAP as well as Flag-CPAP$^{AA}$ and Flag-CPAP$^{EE}$ in which point mutations were introduced into the PLK2 phosphorylation sites serine 589 and serine 595 to become alanines and glutamates, respectively (Chang et al., 2010). The immunoblot analysis revealed that a sufficient amount of the ectopic Flag-CPAP was expressed in the CPAP-depleted cells

(Figure 7A). Flag-CPAP was properly localized at the spindle poles (Figure 7B). At the same time, Flag-CPAP rescued asymmetric spindle poles shown in CPAP-depletion (Figure 7B). Furthermore, the spindle pole asymmetry was also rescued with both Flag-CPAP$^{AA}$ and Flag-CPAP$^{EE}$ (Figure 7B). I counted the number of centrioles in the same experimental groups. Both the wild-type Flag-CPAP and Flag-CPAP$^{EE}$ rescued the number of centrioles to the control level (Figure 8). However, as reported previously, the centriole duplication was not rescued with Flag-CPAP$^{AA}$ (Figure 8). However, most of the Flag-CPAP$^{AA}$-rescued cells had symmetric spindle poles. This suggests that spindle pole asymmetry in CPAP-depleted mitotic cells is independent of CPAP function for procentriole assembly.

**Centriole maturation defects in the young mother centriole of CPAP-depleted cells**

In previous results, PCM was determined by mother centriole not daughter centriole. In fact, I showed that the wild type as well as phospho-resistant and –mimetic mutants of CPAP (CPAP$^{AA}$ and CPAP$^{EE}$) rescued PCM asymmetry regardless of the presence or absence of daughter centrioles (Figures 7B and 8). I asked what differences the mother centrioles at each spindle pole make PCM asymmetry. The prominent difference between mother and daughter centriole is appendage structure at distal part of mother centriole. In fact, the distal and subdistal appendages are markers for centriole maturation (Paintrand et al., 1992; Vorobjev and Chentsov Yu, 1982). I generated a ninein-specific polyclonal antibody as a marker for subdistal appendage (Mogensen et al., 2000; Figure 9). I produced ninein antibody with the fragment (381-689 amino acid residues) (Fig 9A). The rabbit antiserum was affinity-purified

and used for immunoblot analysis. As reported previously, the ninein-specific band of 240 kDa in size was detected in the HeLa cell lysates (Bouckson et al., 1996; Fig. 9B)

In order to determine a precise localization of ninein within the centriole, cells were co-immunostained with the ninein and centrin2 antibodies. Ninein was localized only one of two unduplicated centrioles in G1 phase cells. Ninein was detected at the proximal part as well as distal part of the mother centriole as a ring or three dots. A second ninein signal appeared as a dot at the daughter centriole in a late G1 stage (Figure 10A). The strong and weak ninein signals were placed at the old and young mother centrioles, respectively (Figure 10). This staining pattern was maintained until the young mother centriole became mature at a late G2 phase. Next I observed ninein patterns during the cell cycle. I performed immunostaining analysis with HeLa cells whose cell cycle was synchronized with a double thymidine block and release. The γ-tubulin signals were detected as a single dot in G1 phase cells. The second γ-tubulin dot became visible beginning from S phase and prominent at G2 and M phase cells. Ninein formed a ring or three distinct dots at the centrosome in G1 phase cells. A ring-like structure of ninein was prominent at the strong γ-tubulin staining and a tiny dot of ninein also appeared at the weak γ-tubulin signal in S phase cells. The two ring-like signals of ninein were observed in the G2 phase as young mother centrioles are matured having appendages, and signals became weaker in the M phase centrosomes (Figure 10B). These results suggest that ninein is primarily localized at mature, mother centrioles (Lin et al., 2006; Ou et al., 2002).

Using this ninein antibody, I observed structural maturity of the mother centrioles in control and CPAP-depleted cells. The maturity of young mother centriole

was determined by two ring shape of ninein signal at G2 phase. The ninein signals were detected at the cyclinB1-positive G2 cells, since they became weak and dispersed in M phase cells (Ou et al., 2002). The results showed that most of control cells had two ninein rings which represent two mother centrioles have ninein proteins at its appendages. In CPAP-depleted cells, however, the number of cells with two intact ninein rings was significantly reduced. Instead, over 30% of the CPAP-depleted cells included an intact ninein ring with a dot which represents an immaturity of centriole appendage (Figure 11). These results support the notion that CPAP is required for maturation of the young mother centriole.

I previously showed the similar result with appendage protein Cenexin1 (data not shown). Young mother centriole in CPAP-depleted cells lacks Cenexin1 signal. This result supports that CPAP is also critical for maturation of young mother centriole, in addition to centriole assembly. Cenexin1 is critical for centrosomal recruitment of γ-tubulin (Soung et al., 2006). To know appendage itself affects PCM recruitment, cenexin1 was depleted with siRNA transfection (Figure 12). In cenexin1 knockdown, cenexin1 signals at both spindle poles were diminished, but it was slightly diminished at one spindle pole and absent of the other spindle pole (Figure 12A). At the same time, the γ-tubulin signals were reduced at both ends of spindle poles, but not as much as CPAP depletion (Figure 12B). And the percent of mitotic cells with asymmetric spindle pole was slightly increased in cenexin1-depleted cells but not as much as in CPAP-depleted cells (Figure 12C). These results reveal that appendage itself also functions in PCM recruitment, however asymmetric spindle pole and severe reduction in PCM is due to CPAP function in addition to appendage.

## Centriole size in CPAP-depleted cells

*C. elegans* SAS-4 is essential for centriole elongation as *sas-4* mutants include variable sizes of centrioles (Kohlmaier et al., 2009). Ectopic expression of human CPAP lengthens centrioles, suggesting that CPAP is also involved in centriole elongation (Kohlmaier et al., 2009; Schmidt et al., 2009; Tang et al., 2009). To test whether centriole length determines PCM asymmetry of CPAP-depleted cells or not, I examined the centriole size using a super-resolution microscope. Metaphase centrioles of control HeLa cells were immunostained with the CEP135 and CP110 antibodies as proximal and distal end markers, respectively, and the distance between two markers were determined. SAS6 was also immunostained to distinguish the procentriole from the mother centriole. Average distances of the CEP135 and CP110 signals in mother and procentriole were 360 and 480 nm, respectively (Figure 13A). This numbers are smaller than actual length of mother (513 nm) and daughter (400 nm) centrioles as determined by electron microscopes (Guichard et al., 2010). We reasoned that the distance between the centers of the distal and proximal markers should be smaller than actual size of the centriole. With the same reason, the distance between CEP135 and procentriolar CP110 should be larger, the intercentriole gap and the CEP135 signaling center toward the mother centriole (Figure 13A).

I determined the distance between CEP135 and CP110 signals in CPAP-depleted cells. The results showed that the distance in procentrioles was slightly smaller in the CPAP-depleted cells but the sizes of mother centrioles in CPAP-depleted mitotic cells are identical to those of the control cells (Figure 13B). Furthermore, I do not observe any difference in centriole sizes between a pair of

spindle poles. These results suggest that CPAP depletion does not affect the mother centriole length whereas daughter centriole elongation is slightly affected. Therefore, it is likely that centriole size has little effects on asymmetric spindle pole formation.

**Figure 6. Reduced numbers of centrioles in the CPAP-depleted mitotic cells.** The CPAP-depleted cells were co-immunostained with the centrin-2 (green) and γ-tubulin (red) antibodies. The cells were categorized with the number of centrioles at the mitotic spindle poles. Histogram shows that percentage of cells with different centriole numbers in control and CPAP-depleted cells. The color of bar indicates hours after siRNA transfection. For statistical analysis, more than 300 mitotic cells per experimental group were analyzed from three independent experiments.

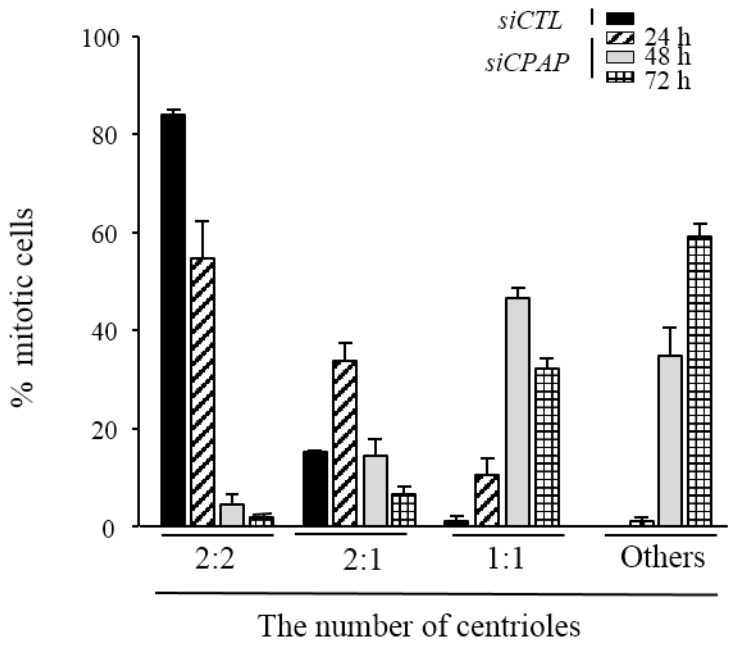
siCTL
siCPAP
24 h
48 h
72 h
100
80
60
40
20
0
% mitotic cells
2:2
2:1
1:1
Others
The number of centrioles

**Figure7. Rescue experiments with the ectopic FLAG-CPAP proteins** (A) HeLa cells were transfected with control (*siCTL*) or CPAP (*siCPAP*) siRNAs, and subsequently with the FLAG-tagged expression vectors (pFLAG-GFP, pFLAG-CPAP, pFLAG-CPAP$^{AA}$ and pFLAG-CPAP$^{EE}$). Expression of the ectopic and endogenous CPAP proteins was confirmed with the immunoblot analysis. (B) The CPAP-rescued cells at mitosis were enriched with a thymidine block and release, followed by the MG132 treatment for 1 h. MG132 is a proteasome inhibitor and blocks transition to anaphase. The cells were immunostained with antibodies specific for FLAG and γ-tubulin. The scale bar represents 10 μm. The mitotic cells with asymmetric distribution of γ-tubulin were determined by comparing relative γ-tubulin intensities between the spindle pole pair. Spindle poles were determined as asymmetric when the intensity of one pole was at least 1.5 fold higher than the other pole within one cell. More than 300 cells were analyzed from four independent experiments, and the results are presented as means and standard errors. *, $P<0.05$

**A.**

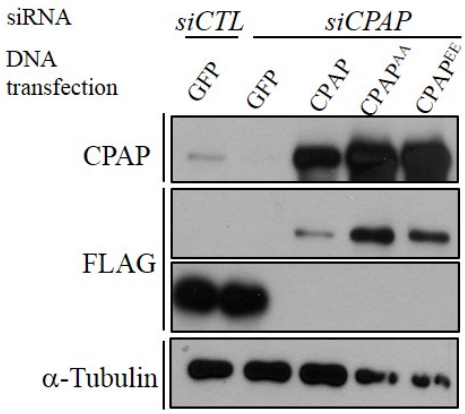
siRNA
siCTL
siCPAP
DNA transfection
GFP
GFP
CPAP
CPAPAA
CPAPEE
CPAP
FLAG
α-Tubulin

**B.**

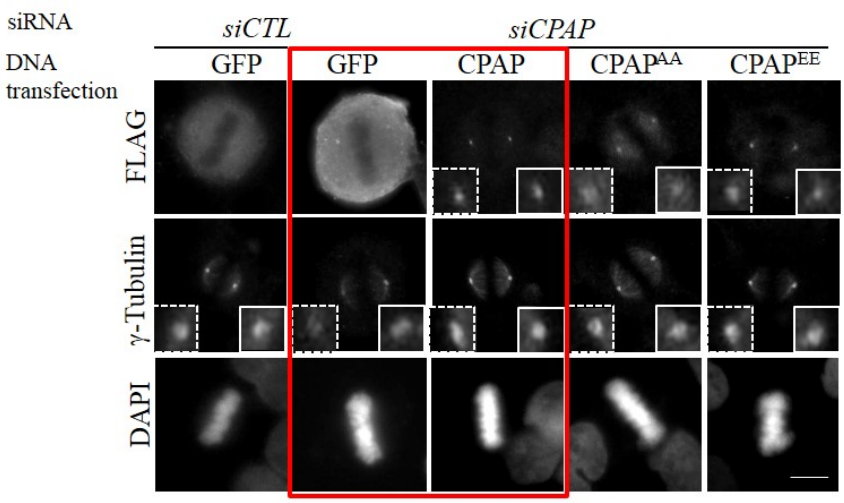
siRNA
siCTL
siCPAP
DNA transfection
GFP
GFP
CPAP
CPAPAA
CPAPEE
FLAG
γ-Tubulin
DAPI

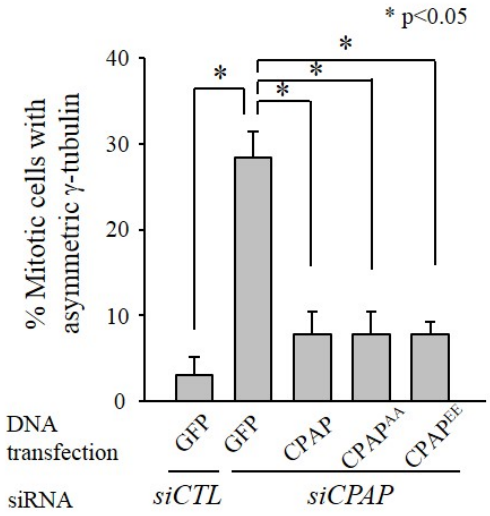
* p<0.05
% Mitotic cells with asymmetric γ-tubulin
40
30
20
10
0
DNA transfection
GFP
GFP
CPAP
CPAPAA
CPAPEE
siRNA
siCTL
siCPAP

**Figure 8. Centriole duplication was rescued in CPAP$^{WT}$ but not in CPAP$^{AA}$ mutant.** The CPAP-rescued cells were immunostained with the antibodies specific for FLAG and centrin-2. The centriole number was determined at the mitotic spindle poles. For statistical analysis, more than 200 mitotic cells per experimental group were analyzed from three independent experiments.

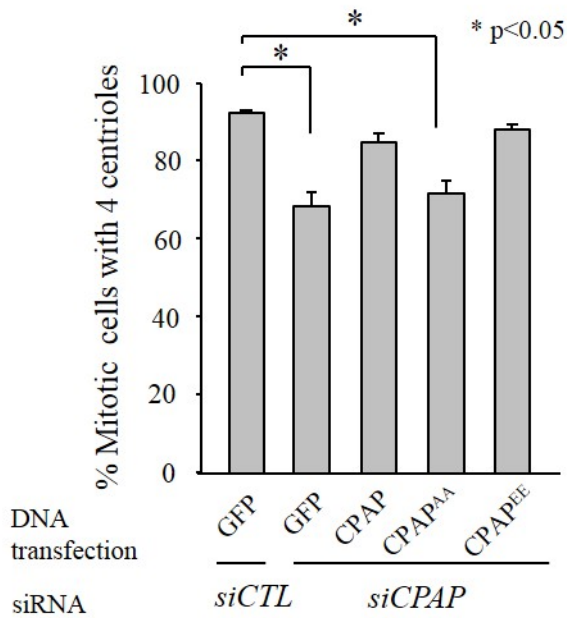
*
*
* p<0.05
% Mitotic cells with 4 centrioles
100
80
60
40
20
0
GFP
GFP
CPAP
CPAPAA
CPAPEE
DNA transfection
siRNA
siCTL
siCPAP

**Figure 9. Generation of ninein antibody.** (A) Ninein is a 2096 amino acid-long protein. The 381-689 fragment of ninein (solid bar) was used for generation of the ninein antibody. (B) HeLa lysates were subjected to immunoblot analysis with the affinity-purified ninein antibody. An estimated size of ninein is about 240 kDa)

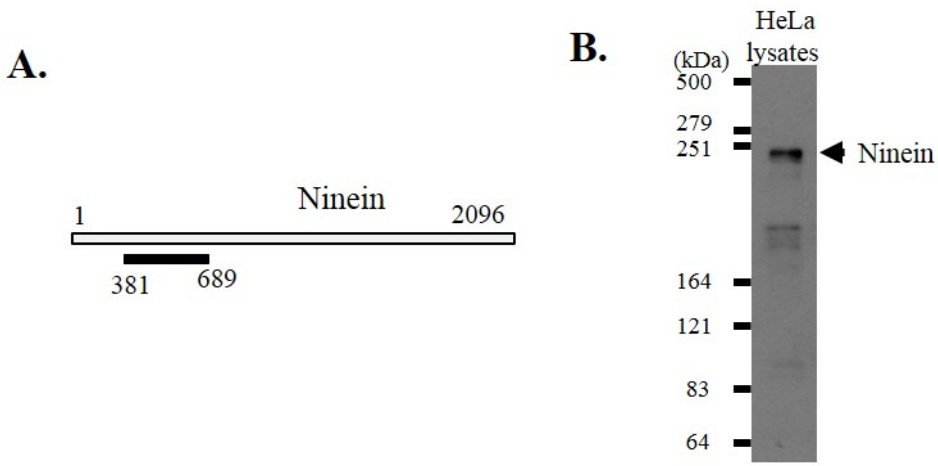
A.
Ninein
1
2096
381
689
B.
HeLa
lysates
(kDa)
500
279
251
164
121
83
64
Ninein

**Figure 10. Patterns of the ninein signal during the cell cycle progression.** (A) Asynchronous HeLa cells were stained with centrin2 (green) and ninein (red) antibodies. Scale bar, 10 ㎛. (B) HeLa cells were synchronized at G1/S, S, G2 and M phase by double thymidine block and release. The time point of release is 0, 4, 8 and 12 h, respectively. Cells were stained with ninein and γ-tubulin antibodies.

**A.**

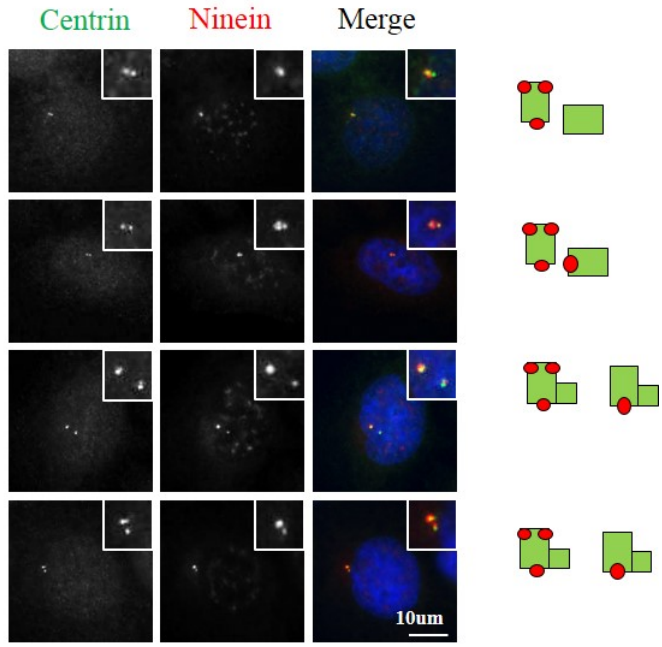


**B.**

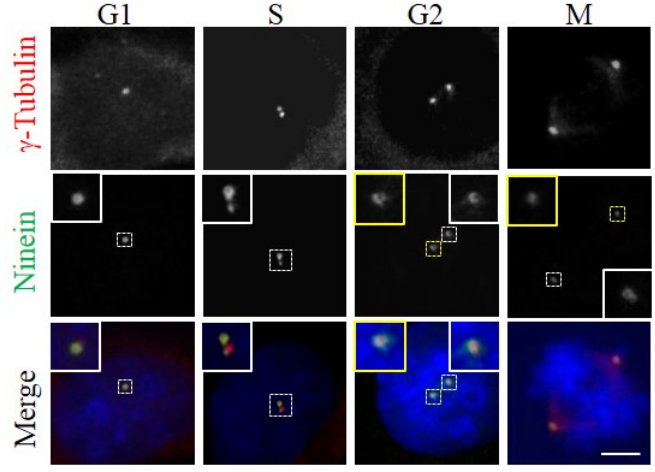

**Figure 11. Abnormal ninein distribution in CPAP-depleted mitotic cells.** (A) The cell cycle of CPAP-depleted cells was synchronized at G2 phase with a double thymidine block and release. The cells were placed on ice for 90 min to disrupt microtubules and co-immunostained with the acetylated-tubulin (red), cyclin B1 (red) and ninein (green) antibodies. (B) The ninein staining patterns at the spindle poles were categorized into four groups: a paired ring, a ring with a bar, a single ring and disrupted. Over 300 cells were analyzed from three independent experiments.

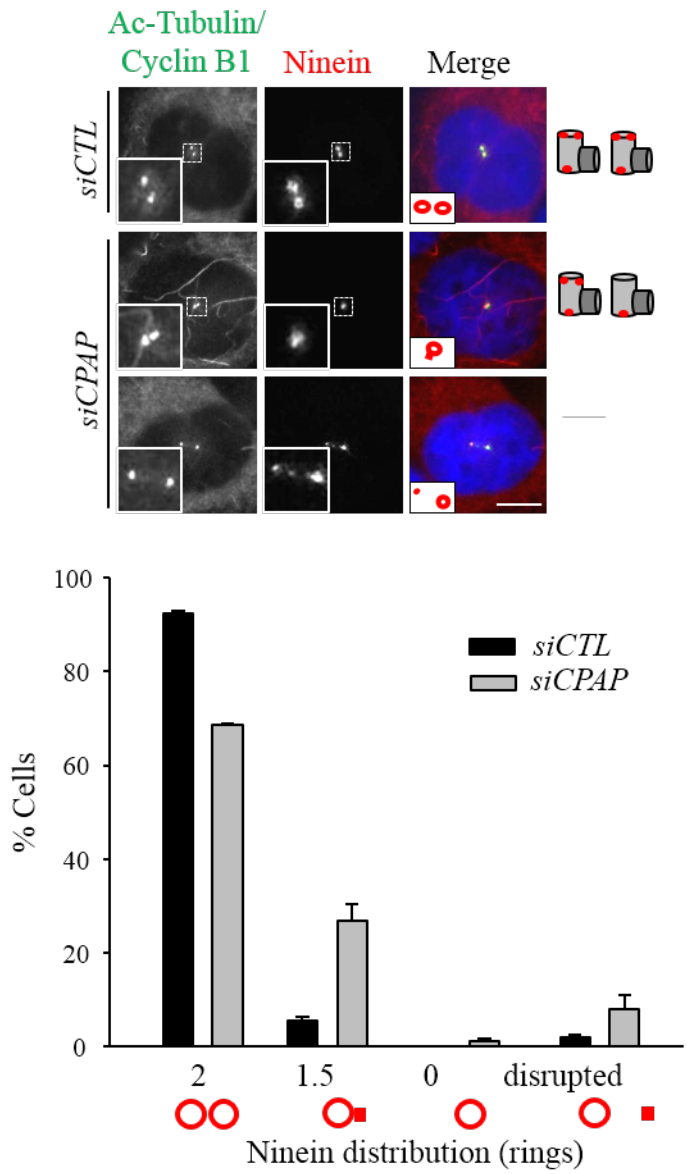
Ac-Tubulin/
Cyclin B1
Ninein
Merge
siCTL
siCPAP
100
80
60
40
20
0
% Cells
siCTL
siCPAP
2
1.5
0
disrupted
Ninein distribution (rings)

**Figure 12. Asymmetric spindle pole phenotype is shown in CPAP-depleted cells, but not in Cenexin1-depleted cells.** (A) Cenexin1-depleted cells were co-immunostained with antibodies specific for Cenexin1 and γ-tubulin. (B) The CPAP- and Cenexin1-depleted cells were co-immunostained with antibodies specific for centrin and γ-tubulin. DNA was stained with DAPI. The scale bar represents 10 μm. Relative γ-tubulin intensities in the mitotic spindle poles were determined at the mitotic spindle poles. Intensity was measured at poles with 2 centrioles. Among two value of intensity in bipolar spindle, I defined poles with higher intensity as poles with old mother centrioles. Over 60 mitotic cells were analyzed in two independent experiments. (C) A difference in intensity greater than 1.5 was defined as an asymmetric distribution. The graph shows that the percent of mitotic cells with asymmetric γ-tubulin distribution was counted in the CPAP- and Cenexin1-depleted cells. Over 200 mitotic cells were analyzed in two independent experiments.

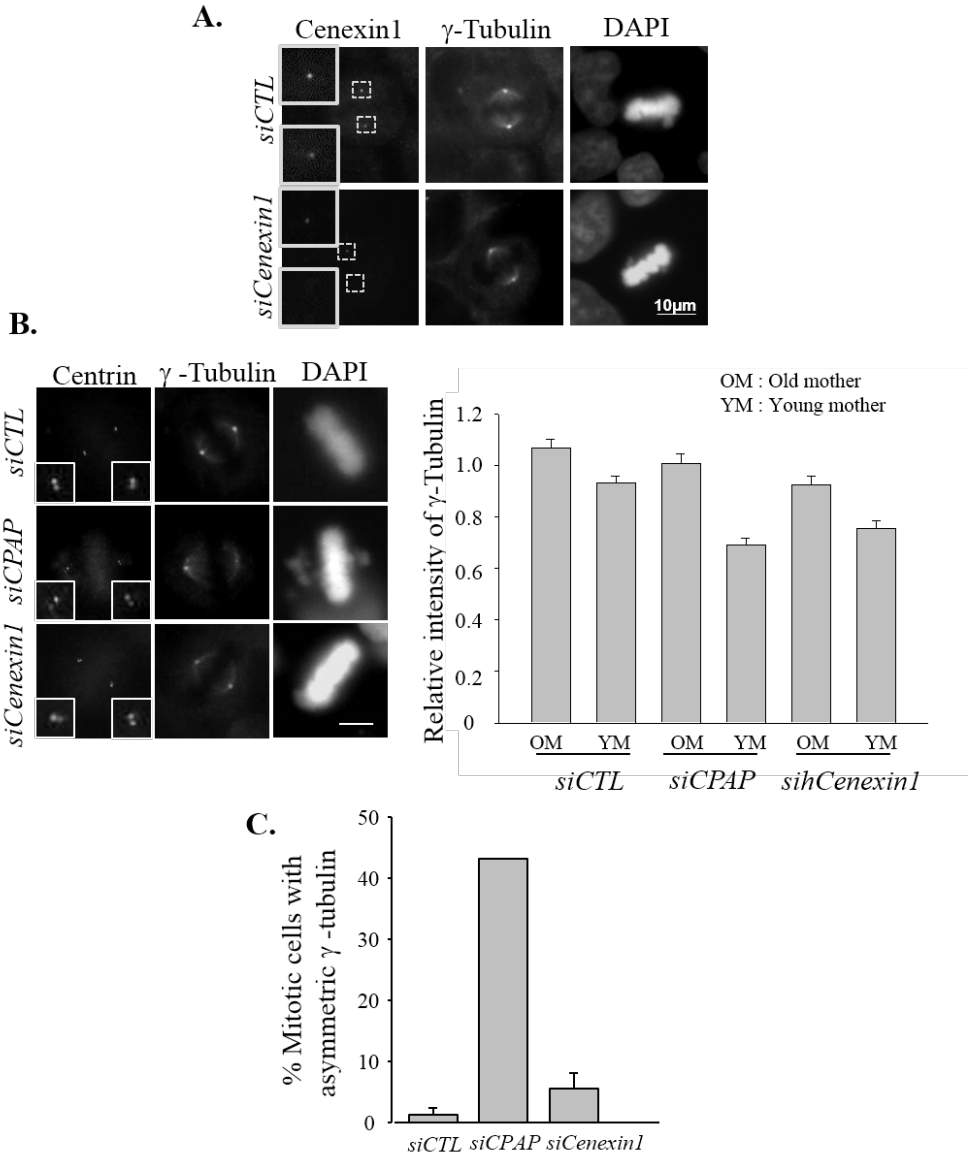
A.
Cenexin1
γ-Tubulin
DAPI
siCTL
siCenexin1
10μm
B.
Centrin
γ -Tubulin
DAPI
siCTL
siCPAP
siCenexin1
OM : Old mother
YM : Young mother
Relative intensity of γ-Tubulin
1.2
1.0
0.8
0.6
0.4
0.2
0
OM
YM
OM
YM
OM
YM
siCTL
siCPAP
sihCenexin1
C.
% Mitotic cells with asymmetric γ -tubulin
50
40
30
20
10
0
siCTL
siCPAP
siCenexin1

**Figure 13. Determination of centriole lengths in CPAP-depleted mitotic cells.** (A) Mitotic HeLa cells were co-immunostained with antibodies specific to CEP135 (red), CP110 (green) and SAS-6 (green), and the spindle poles were observed with a super-resolution microscope. Distance between red (CEP135) and green (CP110) dots were determined. Procentrioles were identified with two consecutive green dots. Nineteen centrioles were analyzed and the data were presented as means and standard errors. (B) The distance between CEP135 (red) and CP110 (green) signals was determined in CPAP-depleted mitotic cells. Over 60 centrioles were analyzed per experimental group from three independent experiments. *, $P<0.05$

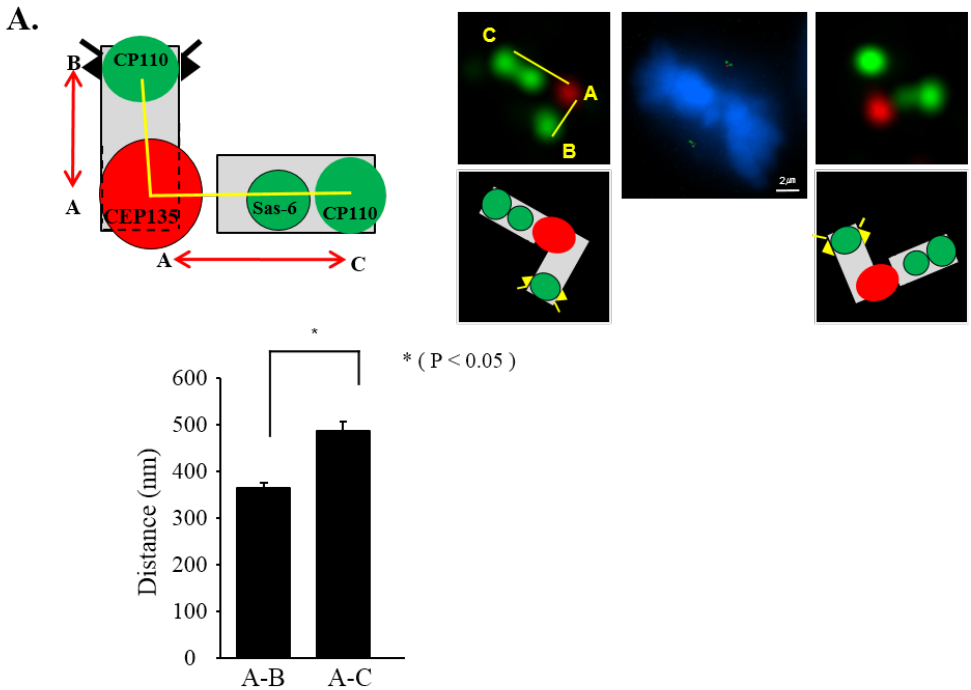
A.
B
CP110
A
CEP135
Sas-6
CP110
A
C
C
A
B
2μm
* ( P < 0.05 )
Distance (nm)
600
500
400
300
200
100
0
A-B
A-C
B.
* ( P < 0.05 )
Distance (nm)
600
500
400
300
200
100
0
siCTL
siCPAP
siCTL
siCPAP
A-B
A-C

**Figure 14. Model.** Depletion of CPAP may result in defects in centriole duplication. In addition, the young mother centriole in CPAP-depleted cells is still immature even in the M phase. Defects of mother centriole maturation is shown in both case, with procentriole and without procentriole. The immaturity of young mother centriole results in the absence of distal and subdistal appendages in the young mother centriole, which may cause an asymmetric spindle pole in CPAP-depleted cells.

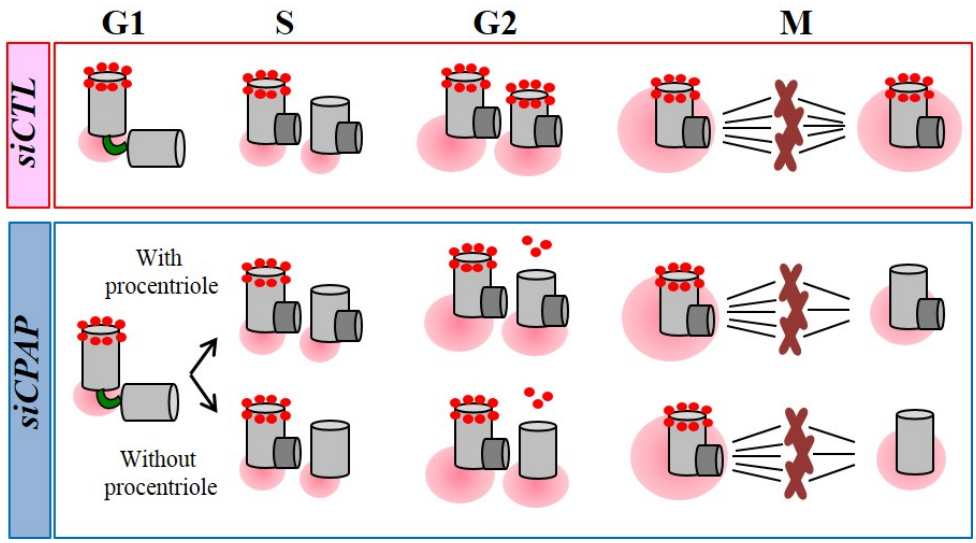
G1
S
G2
M
siCTL
siCPAP
With procentriole
Without procentriole

# Discussion

In this study, I investigated CPAP functions in bipolar spindle formation during mitosis. Prolonged depletion of CPAP resulted in centriole reduction and monopolar spindle formation (Kohlmaier et al., 2009; Schmidt et al., 2009; Tang et al., 2009). At the same time, asymmetry was observed even in bipolar spindle poles with intact number of centrioles. *C. elegans* SAS-4 is also known to be critical for spindle pole formation as well as for centriole duplication. The *sas-4* mutants contain small centrioles, and the amount of PCM is proportionally reduced with respect to the centriole length (Kirkham et al., 2003). In HeLa cells, the mother centriole lengths in CPAP-depleted cells are more or less identical to those of control cells. Therefore, the spindle pole asymmetry is not likely due to the size difference of mother centrioles in CPAP-depleted cells. Rather, I propose that the mother centrioles are not fully matured in the CPAP-depleted cells and, as a result, the microtubule organizing activity of the spindle pole with an immature mother centriole is not sufficiently extended (Figure 11, 12). I believe that spindle pole asymmetry in CPAP-depleted cells is independent of procentriole assembly, because the PLK2 phosphorylation-resistant CPAP mutant did not rescue the centriole duplication activity but did rescue the phenotype of asymmetric spindle pole formation (Figure 7, 8).

This is the first report that CPAP is required for mother centriole maturation in mammalian cells, as evidenced by the absence of distal and subdistal appendage proteins in CPAP-depleted cells. The distal and subdistal appendages are believed to have roles in microtubule anchorage and in primary cilia formation (Cajanek and Nigg,

2014; Ibrahim et al., 2009; Kodani et al., 2013). The selective absence of centriolar appendages at the young mother centrioles may be responsible for asymmetric spindle pole formation in CPAP-depleted cells (Figure 12C). However, in my observation CPAP depletion results more prominent phenotype in $\gamma$-tubulin recruitment and spindle pole asymmetry (Figure 12B, C). It remains to be determined whether CPAP directly participates in appendage formation or not. It was reported that *Drosophila* SAS-4 scaffolds the pre-assembled cytoplasmic complexes of PCM and tethers them to the centrosome (Gopalakrishnan et al., 2011; Zheng et al., 2014). Therefore, it is possible that CPAP is indirectly involved in the appendage formation by recruiting PCM components which are essential for appendage formation in the young mother centriole.

In brain development, neural progenitor cells divide with vertical division plane to increase their own population and subsequently divide with horizontal division plane to produce differentiated cells. Switching spindle orientation should be a tightly controlled process for the production of neural progenitor pool and differentiated cells at the right moment. It is thought that centrosome is involved in spindle orientation. Especially, centriole maturation is considered an important factor for stem cell differentiation as shown in a report that ninein knockdown results in the premature depletion of progenitors during cortex development in mice (Shinohara et al., 2013; Wang et al., 2009). Here, I observed that the spindle poles in CPAP-depleted cells become asymmetric and the young mother centrioles in CPAP-depleted cells are structurally immature even until mitosis. My results predict that neural stem cells in *CPAP* mutant individuals might prematurely initiate asymmetric division,

which causes a reduction in the stem cell population and subsequent reduction of the differentiated cell population. My results suggest that defects in mother centriole maturation may be a reason why microcephaly is derived from *CPAP* mutations.

# Chapter 2

# PLK4 phosphorylation of CP110 is critical for centriole duplication.

# Abstract

PLK4 plays a central role in the initiation of centriole assembly. However, the key substrates of PLK4 in centriole assembly remain to be investigated. Here, I demonstrated that CP110 was phosphorylated by PLK4 in vivo. PLK4′s phosphorylation of CP110 occurred in cell cycle stage-specific, in that its phosphorylation was peaked at metaphase and significantly decreased at telophase. The phospho-resistant mutant of CP110 inhibited centriole duplication, while the phospho-mimetic mutant of CP110 induced centriole duplication in PLK4-depleted cells. However, the phospho-mimetic mutant of CP110 could not induce centriole duplication in the SAS-6- and CPAP-depleted cells. The phospho-CP110 was recruited to the proximal end of the daughter centrioles at an early stage of centriole assembly. Based on these results, I propose that PLK4 phosphorylation of CP110 is a critical step for stabilization of the recruited centriole components.

**Keywords**: PLK4, CP110, centriole duplication, phosphorylation

# Introduction

Centrosomes are composed of two centrioles that are embedded in pericentriolar materials (PCM). Like chromosome, centrioles are duplicated during G1/S phase and then segregated to each daughter cell. Strict control of centriole duplication is important for normal cell division and proliferation. Centriole duplication mechanism is highly conserved in many species. In mammals, PLK4 is a key regulator of centriole duplication, and recruitment of PLK4 appears to be a critical event that triggers the subsequent processes (Bettencourt-Dias et al., 2005; Habedanck et al., 2005). Moreover, hSas-6, STIL, CEP135, CPAP and CP110 are indispensable for centriole assembly.

Polo-like kinase 4 (PLK4) plays a key role in initiating centriole assembly. Overexpression of PLK4 induces centriole overduplication, and its knockdown disrupts procentriole assembly (Bettencourt-Dias et al., 2005; Rodrigues-Martins et al., 2007). This indicates that protein level of PLK4 tightly regulates centriole assembly process. PLK4 stability is regulated by auto-phosphorylation in trans and $SCF^{\beta TrCP}$ dependent degradation (Guderian et al., 2010; Holland et al., 2012). Recently, the mechanism of PLK4 recruitment was reported. Author suggested that CEP192 and CEP152 spatiotemporally regulate PLK4 recruitment and localization through ordered interaction (Kim et al., 2013). Although PLK4 plays a crucial role in centriole assembly, critical substrates of PLK4 involved in the centriole initiation mechanism still need to be identified.

GCP 6, which is a member of γ-TuRC, is reported as a PLK4 substrate and

required for centriole duplication (Bahtz et al., 2012). FBXW5 E3 ubiquitin ligase is also phosphorylated and negatively regulated by PLK4. $SCF^{FBXW5}$ complex suppress Sas6 ubiquitination and degradation. So PLK4 regulates centriole re-duplication regulating Sas-6 level through $SCF^{FBXW5}$ phosphorylation. FBXW5 is also substrate of PLK4 and functions in sas6 degradation, which is a major component of the cartwheel structure. STIL is also a key regulator of centriole assembly, forming a scaffold for recruiting hSas-6. Recently, Kitagawa group showed that phosphorylation of STIL by PLK4 facilitates the STIL/hSAS-6 interaction and recruitment of sas-6 to the centrioles (Ohta et al., 2014).

CP110 was initially reported as a CDK2 substrate (Chen et al., 2002), and is required for centriole overduplication. However, CP110 knockdown did not result in centriole reduction. The possible explanation for this is that, if CP110 is functioning catalytically or structurally, residual protein after knockdown may be sufficient to allow for a single duplication but not multiple duplication (Chen et al., 2002). CP110 localized to the distal part of centriole. CP110 is recruited early step and tubulin dimers were inserted underneath a CP110 cap, elongating centrioles. However, exact role of CP110 is elusive. In relationship between PLK4 and CP110, one group showed that both CP110 and Hssas6 are required for PLK4-induced centrosome amplification (Habedanck et al., 2005).

In terms of CP110 function in centriole assembly, the protein level of CP110 is involved in this process. CP110 protein levels are controlled during the cell cycle. This regulation is one of tight control to prevent centriole duplication error. CP110 levels drop in G2/M phase. CP110 is ubiquitinated by SCF cyclin F E3 ubiquitin

ligase and then degraded during G2 phase (D'Angiolella et al., 2010).

CP110 also functions in cilia assembly. CP110 removal at the mother centriole seems to be crucial role in the initiation of ciliogenesis. Two distal proteins CP110 and Cep97 interact each other and negatively regulate cilia assembly (Spektor et al., 2007). And CP110 interacts with CEP290 and suppresses cilia formation (Tsang et al., 2008). CP110 also binds with Kif24 specifically and remodels centriolar microtubules, thereby regulating cilia assembly (Kobayashi et al., 2011).

# Materials and Methods

## Constructs

CP110 cDNA clone was purchased from Kazusa DNA research institute (WWW.Kazusa.or.jp). The full-length human CP110 open reading frame was cloned into 3xFlag vector (Sigma) and TRE vector (Clontech). CP110 phospho-resistant and phospho-mimic mutant constructs were generated by site-directed mutagenesis. GFP open reading frame was also cloned into 3xFlag vector as a control vector.

## Cell culture

HeLa cells and 293T Cells were grown at 37°C and 5% $CO_2$ in high glucose DMEM supplemented with 10% fetal bovine serum. U2OS cells were grown at 37°C and 5% $CO_2$ in McCoy's 5A supplemented with 10% fetal bovine serum.

## Generation of stable cell lines

TRE CP110 WT, 98A and 98E constructs were transfected into HeLa and U2OS tet-on (tetracycline inducible) stable cell line. Stable cells expressing CP110 was selected in 400 μg/ml hygromycine.

## Transfection and RNA interference

*siCP110* (CAC UCC ACU GCA GCA AAG CTT), *siCTL* (scrambled sequence for control) (GCA AUC GAA GCU CGG CUA CTT), *siPLK4* (CUA UCU UGG AGC UUU AUA ATT), *siSAS6* (GCA CGU UAA UCA GCU ACA ATT), *siCPAP* (GGA CUG ACC UUG AAG AGA ATT) were used for RNAi experiments. The siRNAs were transfected into HeLa cells and U2OS cells using RNAi MAX reagents (Invitrogen). Plasmids were transfected with FuGENE HD (Roche). For

siRNA knockdown and DNA overexpression experiment, siRNAs and DNAs were sequentially transfected.

**Antibodies**

Centrobin/Nip2, CEP135, CP110, centrin-2 rabbit polyclonal antibodies were generated and affinity purified against His-Nip2$^{1-523}$, GST-CEP135$^{295-1141}$, CP110$^{1-334}$ GST-Centrin-2$^{1-172}$. Antibodies against γ-tubulin (C-20, Santa Cruz Biotechnology, Inc.) cyclin B1 (GNS1, Santa Cruz Biotechnology, Inc.), Flag (F3165, Sigma), α-tubulin (Abcam), Sas-6 (91.390.21, Santa Cruz Biotechnology), Centrin (20H5, Millipore), phoshpo histon H3 (Millipore) antibodies were purchased. Cdk2 antibody was given from Hwang and Kif 24, Cep97 and Cep76 antibodies were given from Brian David Dynlacht. pCP110$^{S98}$ antibody raised to a phosphopeptide corresponding to residues CRKAPNApSDFDQW. Generated pCP110$^{S98}$ antibody was purified using column purification with phospho- and non phospho-peptides.

**Cell cycle synchronization**

To measure phosphos-CP110 signal during cell cycle (Figure 18), HeLa cells were synchronized at S phase with 2 mM thymidine and then release for 7 h. To increase mitotic cells, 100 ng/ml nocodazole was treated into released cells for 3 h. Mitotic cells were shaken off and then reseeded to coverslip and observed each time point. For centrosome overduplication (Figure 19, 20), U2OS cells were arrested at S phase with 2 mM hydroxyurea (HU) treatment for 48 h. For CP110 degradation experiment (Figure 28), HeLa stable cells were arrested at S phase with 2 mM thymidine for 16 h. And STLC was treated together with thymidine release. To observe APC/C oscillation, Cells were synchronized in G1/S with 2 mM thymidine

for 20 h then released into fresh medium for 4 h. To inhibit Cdk1, cells were treated with 10 nM RO-3306 (Calbiochem).

**Immunoblot analysis**

Cultured HeLa cells were lysed in the sample buffer (50 mM Tris-HCl, pH 6.8, 100 mM dithiothreitol, 2% SDS, 0.1% bromophenol blue, 10% glycerol). Samples were loaded in 8% and 4% polyacrylamide gels and then transferred into nitrocellulose membranes. The membranes were blocked in 5% skim milk in TBST (20 mM Tris, 150 mM NaCl, 0.3% Triton X-100) for 30 min, incubated with antibodies for overnight at 4°C. After washing three times with TBST for 7 min, the membranes were incubated with mouse and rabbit secondary antibodies (1:10,000) for 40 min. After the membranes were washed three times with TBST for 5 min, the peroxidase activity was detected using ECL solutions.

**Immunofluorescence and Microscopy**

For indirect immunocytochemistry, HeLa and U2OS cells were grown on 12-mm coverslips and fixed with cold 100% methanol for 10 min. In some cases, cells were pre-extracted with 0.1% PBST before fixation. The cells were then permeabilized and blocked with 3% BSA in 0.5% PBST for 15 min. Primary antibodies were diluted in 3% BSA in 0.5% PBST, incubated at room temperature for 1 or 2 h and coverslips were washed three times in 0.1% PBST. Secondary antibodies were diluted in 3% BSA in 0.5% PBST, incubated for 30 min at room temperature and washed again three times in 0.1% PBST. For DNA staining, DAPI solution was used at the final step for 4 min. The coverslips were mounted on slides and observed with a fluorescence microscope (Olympus IX51) equipped with a CCD camera (Qicam fast

1394, Qimaging). Images were processed using ImagePro 5.0 (Media Cybernetics, Inc.) and statistic analyzed with Sigma Plot (Systat Software, Inc.).

**Immunoprecipitation**

293T cells were washed with PBS and lysed in in ELB buffer (50 mM HEPES pH 7, 250 mM NaCl, 5 mM EDTA pH 8, 0.1% NP40, 1 mM DTT, 0.5 mM phenylmethylsulfonyl fluoride (PMSFP), 2 μg /ml leupeptin, 2 μg aprotinin, 10 mM NaF, 50 mM β–glycerophosphate and 10% glycerol at 4°C for 30 min). The lysates were on ice for 40 min, and insoluble material was removed through centrifugation for 20 min at 4°C. For immunoprecipitation, cell lysates were incubated with pre-immune serum, as a control, Kif24, CEP97 antibodies for overnight at 4°C. After then lysates were incubated with protein A sepharose beads (Amersham Pharmacia) for 90 min at 4°C. For Flag beads immunoprecipitation, cell lysates were incubated with Flag beads (Sigma) instead of antibodies for 90 min. In both cases, the beads were washed three times with lysis buffer and mixed in SDS sample buffer. Samples were loaded onto a SDS-PAGE gel.

**Super resolution structural illumination microscopy (SR-SIM)**

Sample preparation and dyes were same with previous fluorescence microscopy. Microscope stand : Axio Observer.Z1 SR, fully motorized inverted microscope stand for super resolution microscopy; motorized XY scanning stage 130x100 DC; fast Z-piezo insert for XY scanning stage (sample holders available for standard 3”x1” slides and 36 mm glass-bottom dishes) Detector : Andor iXon 885 EMCCD camera; pixels:1004 x 1002; pixel size: 8 μm x 8 μm; Objectives : “Plan-Apochromat” 63x/1.40 Oil DIC, alpha “Plan-Apochromat” 100x/1,46 Oil DIC

# Results

## Generation of the phospho-antibody against phospho-serine 98 of CP110 (pCP110$^{S98}$)

PLK4 is a key kinase in centriole assembly. A previous work in my laboratory revealed that PLK4 specifically phosphorylates serine 98 of CP110 in vitro (Figure 15A). In order to determine phosphorylation of CP110 in vivo, I generated a phospho-antibody specific to phospho-serine 98 of CP110 (pCP110$^{S98}$). To increase specificity to phosphorylated CP110, I carried out column purification with phospho- and non phospho-peptides. As a result, the purified pCP110$^{S98}$ antibody strongly interacted with the phospho-peptide but not with the non-phospho-peptide (Figure 15B).

## PLK4 phosphorylates CP110 in vivo

I performed immunoblot analysis with the pCP110$^{S98}$ antibody. The endogenous CP110 protein was concentrated with immunoprecepitation. A pCP110$^{S98}$ specific band was detected when the cell lysates were immunoprecipitated with the CP110 anti-serum, but not with the preimmune serum (Figure 16). Furthermore, the pCP110$^{S98}$-specific band was absent in the PLK4-depleted cells (Figure 16). These results confirmed the specificity of the pCP110$^{S98}$ antibody. Furthermore, the results support the notion that PLK4 specifically phosphorylates serine 98 of CP110 in vivo.

I performed immunostaining analysis with the pCP110$^{S98}$ antibody. A specific signal of pCP110$^{S98}$ was detected at the centrosome (Figure 17). Intensity of the phospho-specific signal was significantly reduced in the PLK4-depleted cells

(Figure 17). The results indicate that CP110 is phosphorylated by PLK4 in vivo and localized at the centrosome.

## Cell cycle specificity in the phosphorylation of CP110

The centrosomal pCP110$^{S98}$ levels were determined with the pCP110$^{S98}$ antibody in the HeLa cells whose cycle was synchronized with the thymidine and nocodazole block and release. The results showed that the centrosomal intensity of pCP110$^{S98}$ increased when the cells approached to M phase (Figure 18). The centrosomal pCP110$^{S98}$ signal peaked at metaphase and then significantly decreased at telophase (Figure 18). Phosphorylation of CP110 correlates with the PLK4 activity during the cell cycle (Cunha-Ferreira, 2009; Rogers, 2009).

## Centriole overduplication was inhibited with CP110$^{S98A}$

It is known that centrosomes are overduplicated in U2OS cells whose cell cycle is arrested at S phase with hydroxyurea (HU). CP110 is known to be essential for centrosome overduplication in S phase-arrested U2OS cells (Chen et al., 2002). In order to examine if the phosphorylation of CP110 is important for centrosome overduplication, I depleted endogenous CP110 with siRNA transfection, and transiently expressed Flag-CP110, Flag-CP110$^{S98A}$ (phospho-resistant mutant) and Flag-CP110$^{S98E}$ (phospho-mimetic mutant). The cells were treated with hydroxyurea for 72 h, and then immunostained with antibodies specific to Flag and γ-tubulin. As expected, about 60% of the control cells contained overduplicated centrosomes and this number was reduced to 20% in CP110-depleted cells (Figure 19). The cells with overduplicated centrosomes increased up to the control levels in Flag-CP110 and Flag-CP110$^{S98E}$–rescued cells (Figure 19). However, Flag-CP110$^{S98A}$ did not rescue

the phenotype, suggesting that specific phosphorylation of CP110 is required for centriole overduplication (Figure 19).

In order to determine disengagement of the overduplicated centrioles in S phase arrested cells, I immunostained the cells with the CEP135 antibody. The results showed that about 60% of the control cells included more than 2 CEP135 dots and this number was reduced to 30% in CP110 depleted cells (Figure 20). This phenotype was rescued with the wild type Flag-CP110, but not with the Flag-CP110$^{S98A}$ (Figure 20). These results suggest that specific phosphorylation of CP110 induces centriole disengagement in S phase-arrested cells.

## APC/C oscillation in prolonged G2 phase

I observed premature centriole disengagement in S phase-arrested cells (Figure 20). In normal centrosomal cycle, centriole disengagement is closely related to PLK1 activity and anaphase-promoting complex (APC/C)-dependent separase activity. It was thought that premature centriole disengagement results from untimely activation of (APC/C) in cells whose cycle was arrested at G2 phase for a long period (Prosser et al., 2012). Therefore, I examined APC/C activity in the G2 phase-arrested cells with RO3306, which is a highly selective Cdk1 inhibitor (Vassilev et al., 2006). The APC/C activity was indirectly determined by the cellular levels of cyclin B1, which is a substrate of APC/C. In control cells, cyclin B1 began to decrease at 18 hours after RO3306 treatment, suggesting that APC/C became activated at this time point (Figure 21). However, no such decrease of the cyclin Bl level was observed in CP110-depleted cells, suggesting that APC/C is not activated in the CP110-depleted cells (Figure 21).

I indirectly determined the APC/C activity in the Flag-CP110$^{S98A}$ and Flag-CP110$^{S98E}$–expressing cells. I observed fluctuation of cyclin B1 level in all stable cell line (Figure 22). So from this result, I conclude that defects in overduplication in CP110 phospho-resistant mutant is not due to a block of the APC/C oscillation (Figure 22).

## PLK4 phosphorylation of CP110 is essential for procentriole assembly

PLK4 is a critical kinase for initiation of the centriole assembly. In fact, centrioles are not duplicated in PLK4-depleted cells (Figure 23). I examined importance of PLK4 phosphorylation of CP110 in centriole assembly using the phospho-mimetic mutant of CP110 (Flag-CP110$^{S98E}$). The results showed that ectopic expression of Flag-CP110$^{S98E}$ in PLK4-depleted cells enhanced centriole duplication up to the control levels (Figure 23). These results suggest that PLK4 phosphorylation of CP110 is a critical step in centriole assembly.

I performed the rescue experiments with U2OS cells which stably expressed CP110 proteins. PLK4 was depleted with siRNA transfection, and hydroxyurea was treated to arrest the cells at S phase. Thirty-six hours after the siRNA transfection, the cells were immunostained with the centrin antibody to determine centriole number. As expected, PLK4 depletion reduced centriole duplication significantly (Figure 24). The centriole duplication rate was rescued with Flag-CP110$^{S98E}$, but not with Flag-CP110 or Flag-CP110$^{S98A}$ (Figure 24). These results suggest that PLK4 phosphorylation of CP110 may be a prerequisite step for centriole duplication.

## Procentriole formation in the Flag-CP110$^{S98E}$–rescued cells

I immunostained the PLK4-rescued cells with centrobin, a daughter centriole

marker. The results showed that the number of centrobin signals were reduced in PLK4-depleted cells and rescued in the Flag-CP110$^{S98E}$–expressing cells (Figure 25). The results revealed that daughter centrioles are formed in the Flag-CP110$^{S98E}$–expressing cells.

The Flag-CP110$^{S98E}$–expressing cell was able to duplicate centrioles in the PLK4-depleted condition. I examined whether SAS6 is recruited in recruitment or not in this condition. As expected, the SAS-6 signal was greatly diminished in the PLK4-depleted cells (Figure 26). The centrosomal SAS-6 signal was still reduced in the Flag-CP110$^{S98E}$–expressing cell even if the centrioles are efficiently duplicated (Figure 26). These results suggest that Flag-CP110$^{S98E}$ might initiate centriole duplication even with a limited amount of the centrosomal SAS-6.

## CPAP and SAS-6 depletion were not rescued with the phospho-mimetic mutant of CP110

SAS-6 forms the cartwheel structure within the centriole, therefore, it should be recruited at an early stage of centriole assembly process (Azimzadeh, 2010; Keller, 2014). In fact, centrioles were not efficiently assembled in the SAS6-depleted cells (Figure 27). PLK4 is known to play a key role in centriole recruitment of SAS6 (Kim, 2014; Sonnen, 2013). Therefore, it is of interest whether Flag-CP110$^{S98E}$ could rescue phenotypes of the SAS-6 depletion or not. The results showed that the SAS-6 phenotype was not rescued with the wild type and Flag-CP110$^{S98E}$ (Figure 27). These results suggest that PLK4 phosphorylation of CP110 is not a downstream step of the SAS-6 recruitment to the centriole. CPAP is a human homologue of *C. elegans* SAS4 and is essential for the procentriole elongation step (Kohlmaier, 2009). Depletion of

CPAP results in defects in centriole assembly (Figure 28; Kohlmaier, 2009; Schmidt, 2009; Tang, 2009). We examined whether Flag-CP110$^{S98E}$ could rescue phenotypes of the CPAP depletion or not. The results showed that the CPAP phenotype was not rescued with the wild type and mutant Flag-CP110 (Figure 28). These results suggest that PLK4 phosphorylation of CP110 is independent of the CPAP function in centriole assembly.

**Cellular CP110 levels during the cell cycle.**

It is known that CP110 is a cell cycle-regulated protein. CP110 is degraded during G2/M phase and this regulation is involved in centriole assembly (D'Angiolella, 2010; Li, 2013). Proper control of the cellular CP110 levels is important for proper centriole duplication during the cell cycle (D'Angiolella, 2010). We examined the cellular levels of the CP110 point mutants during the cell cycle. I generated HeLa cell lines in which Flag-CP110, Flag-CP110$^{S98A}$ and Flag-CP110$^{S98E}$ were stably expressed. The cells were synchronized with the double thymidine block and release method. As expected, endogenous CP110 decreased when cells enter mitosis (Figure 29). At the same time, ectopic Flag-CP110, Flag-CP110$^{S98A}$ and Flag-CP110$^{S98E}$ also decreased (Figure 29). These results revealed that point mutations at serine 98 residue do not affect CP110 stability during the cell cycle.

**Phosphorylation did not affect CP110 interaction with Kif24 and CEP97**

CP110 controls centriole length and cilia formation (Schmidt, 2009; Tsang, 2008). CP110 interaction with Kif24 and CEP97 is important for initiation of cilia formation. Kif24 binds and depolymerize centriole microtubules (Kobayashi et al., 2011). CEP97 play a role in regulating centriole length and ciliogenesis (Spektor et al.,

2007). I examined importance of CP110 phosphorylation in interaction with Kif24 and CEP97. As expected, Flag-CP110 was coimmunoprecipated with both Kif24 and CEP97 (Figure 30). Flag-CP110$^{S98A}$ was coimmunoprecipated with both Kif24 and CEP97 as well (Figure 30). These results suggest that the specific phosphorylation at serine 98 residue of CP110 has no direct correlation with the CP110 function in centriole length control and cilia formation.

**Centriolar localization of the phosphorylated CP110**

To know where phospho-signal localizes at centrosome, I determined sub-centrosomal localization of phosphorylated CP110 using pCP110$^{S98}$ antibody. The centrosomal intensity of the pCP110 was low in S phase cells (Figure 31A). However, the pCP110 signals in S phase cells were detected at daughter centriole (Figure 31A). To observe more specific localization of pCP110$^{S98}$ signal, I observed it with a super resolution structured illumination microscopy (SR-SIIM). In this observation, pCP110 was localized between the two centrin signals (Figure 31B).

CP110 is known to localize at the distal tip of both centrioles (Kleylein-Sohn, 2007). Since the localization of pCP110$^{S98}$ was different to reported CP110 signals, I observed endogenous CP110 through SIM (Figure 32). In this observation, endogenous CP110 localized strongly at both distal tip of centrioles and weakly between two centrioles. The signal of CP110 at the proximal end of the centrioles was co-localized with the pCP110$^{S98}$ signals (Figure 32).

I examined CP110 localization within the centrosome with a superresolution microscope (Figure 33). As expected, I observed two strong CP110 signals at distal tip of centrioles and an additional weak signal between the centrin signals (Figure 33).

These images suggest that the endogenous CP110 localized not only at the distal part of centriole but also between two centrioles.

**CP110 is recruited to the proximal end of procentrioles at an early stage of centriole assembly**

In order to determine when CP110 is recruited during the procentriole assembly, I immunostained the synchronized HeLa cells with the CP110 antibody. I observed the CP110 signals at daughter centrioles even before the centrin signals (Figure 34A), indicating that CP110 is recruited to the procentriole earlier than centrin. I also observed that a fraction of cells with 4 CP110 dots had a strong SAS6 signals but the others had a weak SAS6 signals (Figure 34B). These results suggest that CP110 is recruited to the procentriole as early as SAS6.

**Figure 15. Generation of a phospho-antibody against serine 98 of CP110 (pCP110$^{S98}$).** (A) Schematic structures of PLK4 and CP110. PLK4 specifically phosphorylates serine 98 of CP110. (B) A phospho-antibody against serine 98 of CP110 was generated and purified with the phospho- and nonphospho-peptides.

**A.**

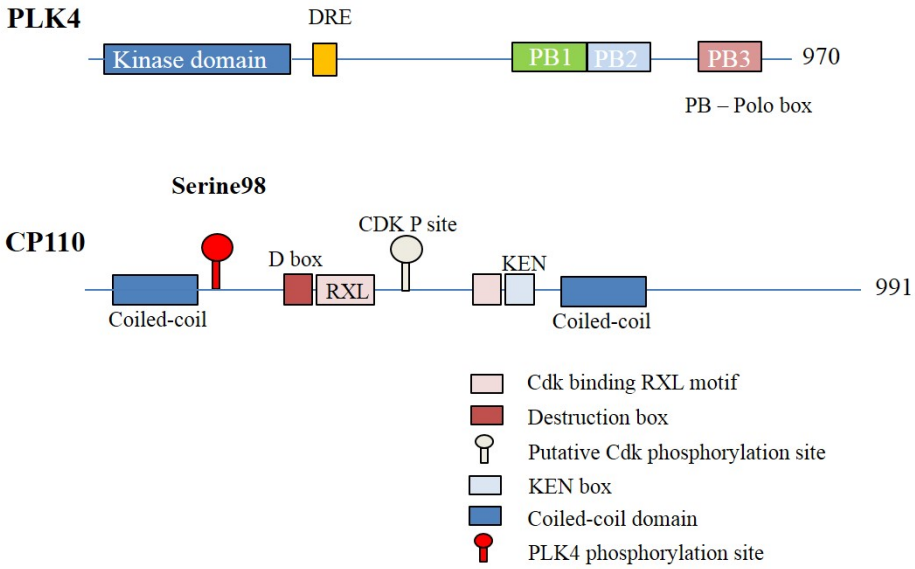
PLK4
DRE
Kinase domain
PB1
PB2
PB3
970
PB – Polo box
Serine98
CP110
CDK P site
D box
RXL
KEN
991
Coiled-coil
Coiled-coil
Cdk binding RXL motif
Destruction box
Putative Cdk phosphorylation site
KEN box
Coiled-coil domain
PLK4 phosphorylation site

**B.**

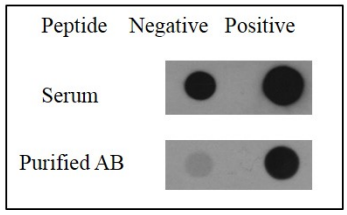
Peptide
Negative
Positive
Serum
Purified AB

**Figure 16. Specific phosphorylation of CP110 in vivo.** The PLK4-depleted HeLa cells were immunoprecipitated with the anti-CP110 serum. The lysates were subjected to immunoblot analysis with antibodies specific to CP110 and pCP110$^{S98}$.

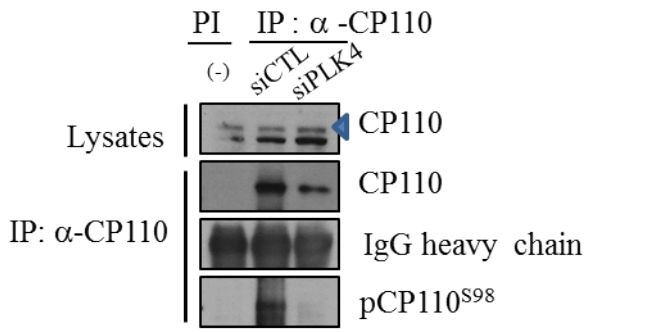


PI : Pre-immune serum

**Figure 17. Immunostaining of the centrosome with the pCP110$^{S98}$ antibody.** The PLK4-depleted HeLa cells were treated with STLC for 3 h and immunostained with antibodies specific to centrin and pCP110$^{S98}$. STLC is an Eg5 inhibitor and induces mitotic arrest. Histogram shows the pCP110$^{S98}$ intensity at each pole. Over 70 poles were measured at each experimental group.*, $P<0.05$

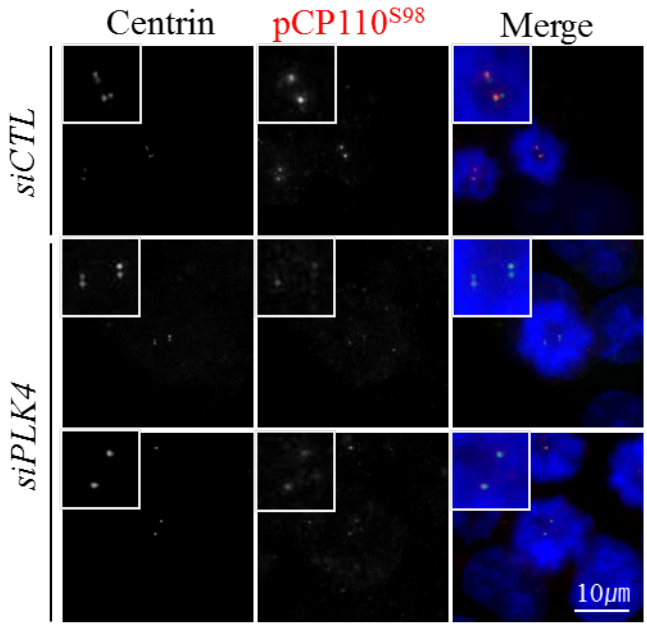
Centrin
pCP110S98
Merge
siCTL
siPLK4
10μm

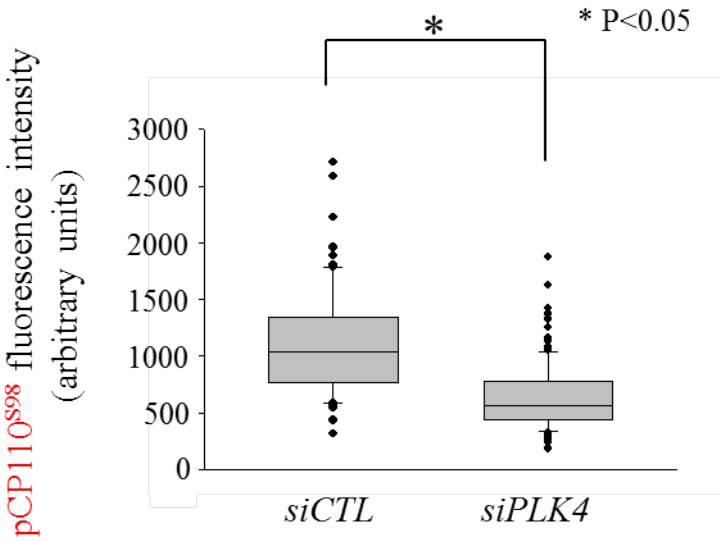
*
* P<0.05
pCP110S98 fluorescence intensity
(arbitrary units)
3000
2500
2000
1500
1000
500
0
siCTL
siPLK4

**Figure 18. Cell cycle stage-specific phosphorylation of CP110.** HeLa cells were synchronized at M phase with the thymidine and nocodazole block. Mitotic cells were shaken off and cultured in a fresh medium. Thymidine is a pyrimidine deoxynuleoside and inhibits DNA replication. Nocodazole is a destabilizer of microtubules and arrest cell cycle at the prometaphase. The cells were fixed at each time point and immunostained with antibodies specific to centrin and $pCP110^{S98}$. The intensities of $pCP110^{S98}$ signals were measured. For statistical analysis, immunofluorescent intensities of at least 20 cells were determined per experimental group. The results are presented as means and standard errors.

HeLa seeding → Thymidine block for 16h → Release(7h) →
Nocodazole treatment (3h) → Shake off mitotic cells → Seeding on coverslip

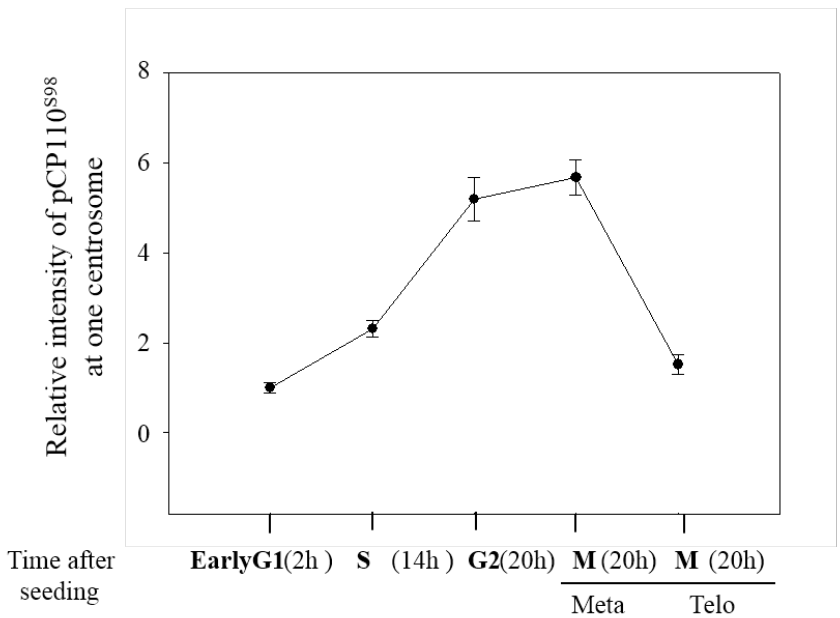

**Figure 19. Centriole overduplication was reduced in U2OS cells rescued with Flag-CP110$^{S98A}$.** The CP110-depleted cells were transfected with the Flag-GFP, Flag-CP110, Flag-CP110$^{S98A}$ and Flag-CP110$^{S98E}$. The cells were treated with hydroxyurea (HU) for 48 h and immunostained with the Flag and γ-tubulin antibodies. Hydroxyurea (HU) is an inhibitor of ribonucleotide reductase and prevents cells from progressing through S phase. Graph shows the percent of cells with three or more γ-tubulin dots. Experiments were repeated 3 times.

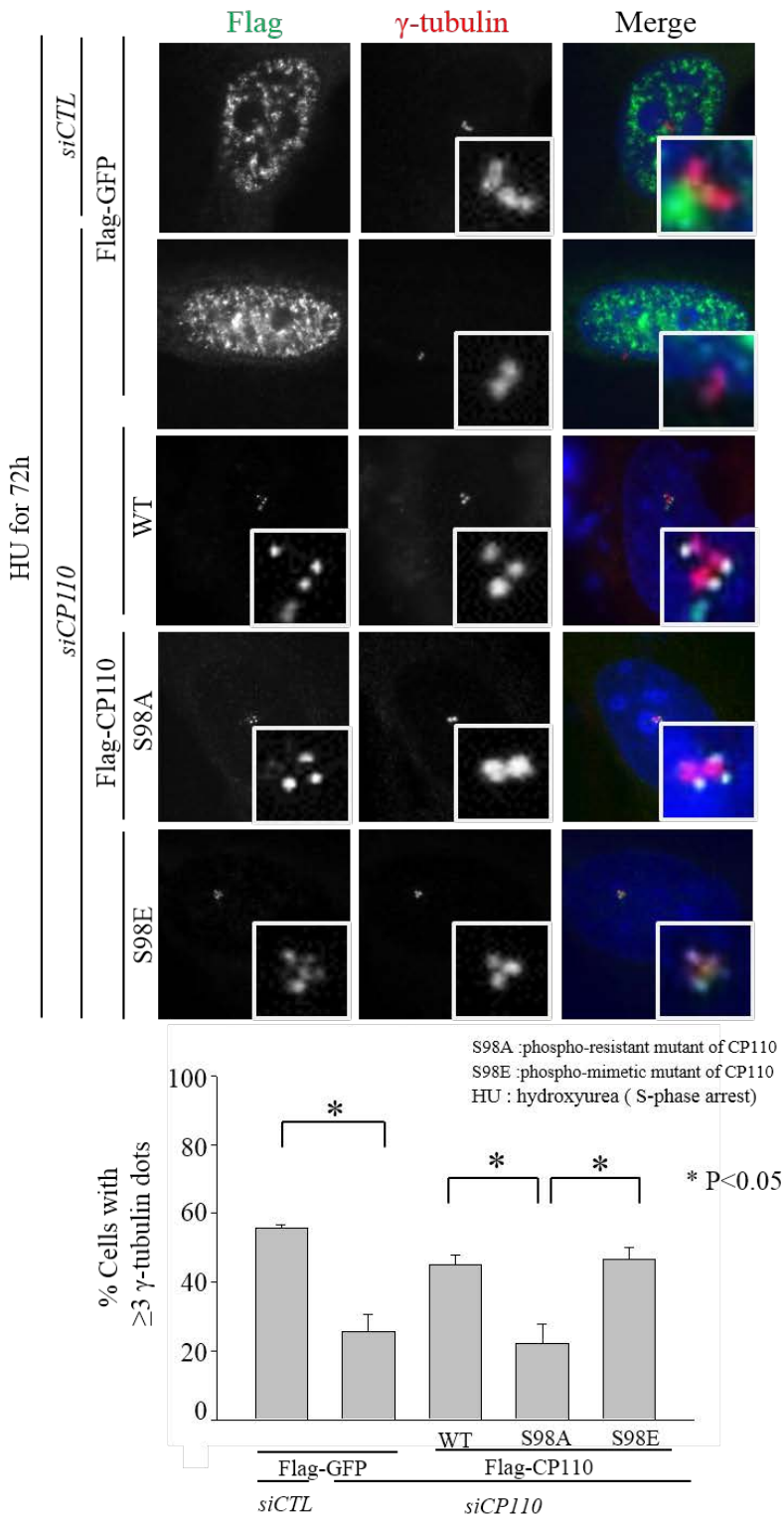
Flag
γ-tubulin
Merge
HU for 72h
siCTL
siCP110
Flag-GFP
Flag-CP110
WT
S98A
S98E
S98A :phospho-resistant mutant of CP110
S98E :phospho-mimetic mutant of CP110
HU : hydroxyurea ( S-phase arrest)
% Cells with ≥3 γ-tubulin dots
100
80
60
40
20
0
*
* P<0.05
WT
S98A
S98E
Flag-GFP
Flag-CP110
siCTL
siCP110

**Figure 20. Centriole disengagement was reduced in U2OS cells rescued with Flag-CP110$^{S98A}$.** The CP110-rescued U2OS cells were immunostained with the antibodies against Flag and CEP135. Graph shows the percent of cells with three or more CEP135 dots. Experiments were repeated 3 times.

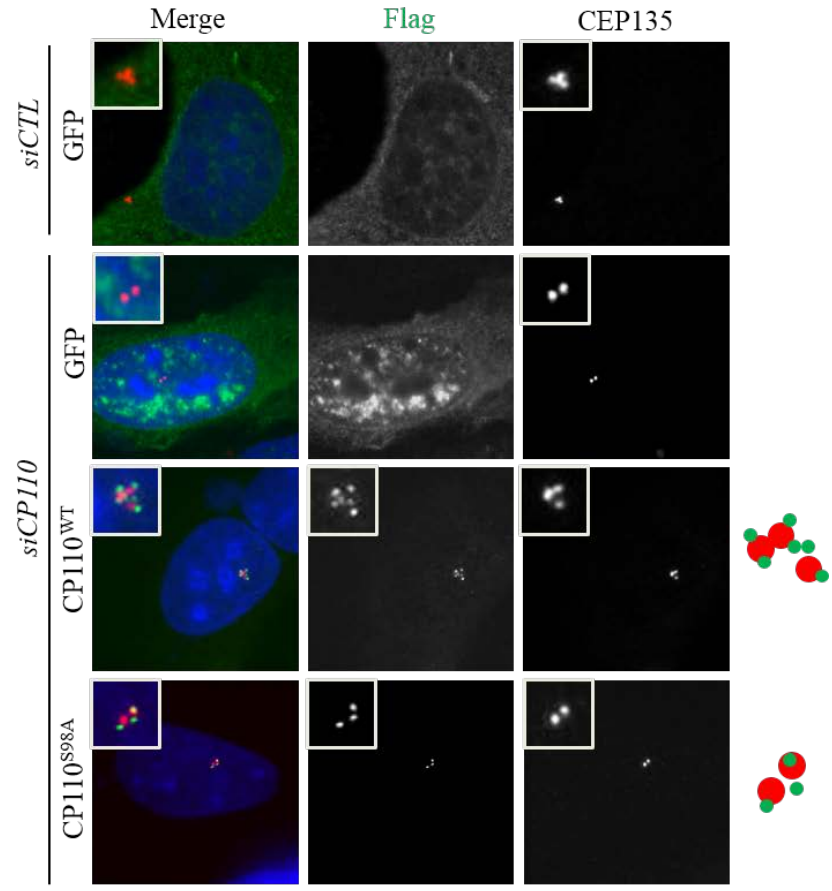
Merge
Flag
CEP135
siCTL
GFP
siCP110
GFP
CP110WT
CP110S98A

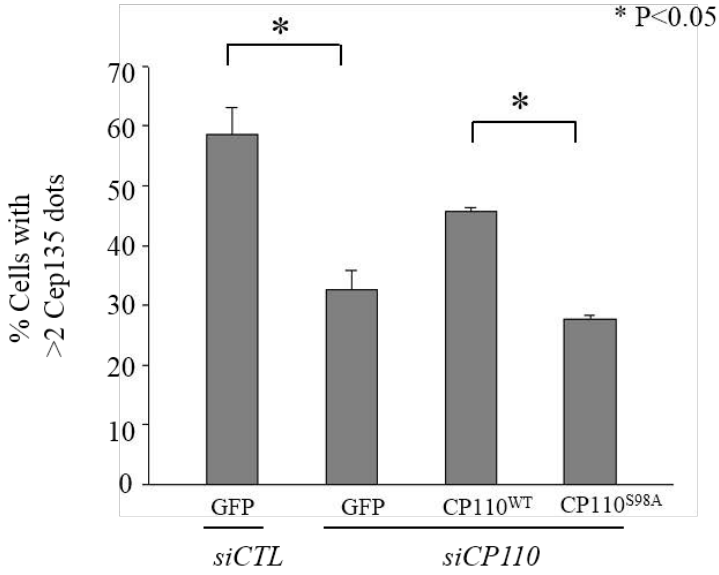
* P<0.05
*
*
% Cells with >2 Cep135 dots
70
60
50
40
30
20
10
0
GFP
GFP
CP110WT
CP110S98A
siCTL
siCP110

**Figure 21. APC/C oscillation during prolonged G2 phase.** (A) Experimental scheme of synchronization protocol for prolonged G2 phase. (B) The CP110-depleted U2OS cells were arrested at G2 phase with selective Cdk1 inhibitor, RO3306 up to 26 h and subjected to immunoblot analysis with the CP110, $\alpha$-tubulin, and cyclin B1 antibodies.

**A.**

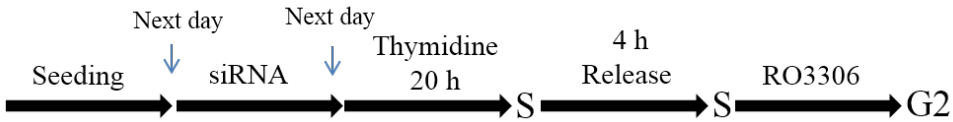
Next day
Next day
Seeding
siRNA
Thymidine
20 h
S
4 h
Release
S
RO3306
G2

**B.**

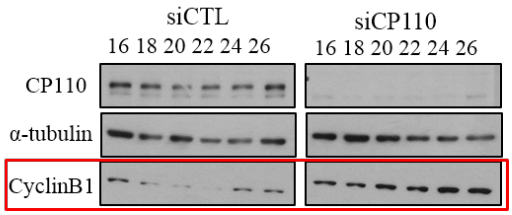
siCTL
16 18 20 22 24 26
siCP110
16 18 20 22 24 26
CP110
α-tubulin
CyclinB1

**Figure 22. APC/C oscillation in Flag-CP110-expressing cells.** The cell cycle of the U2OS stable lines with Flag-CP110, Flag-CP110$^{S98A}$ and Flag-CP110$^{S98E}$ were synchronized with the thymidine and RO3306 block and release. The cells were subjected to immunoblot analysis with the antibodies specific to CP110, Flag, $\alpha$-tubulin, and cyclin B1.

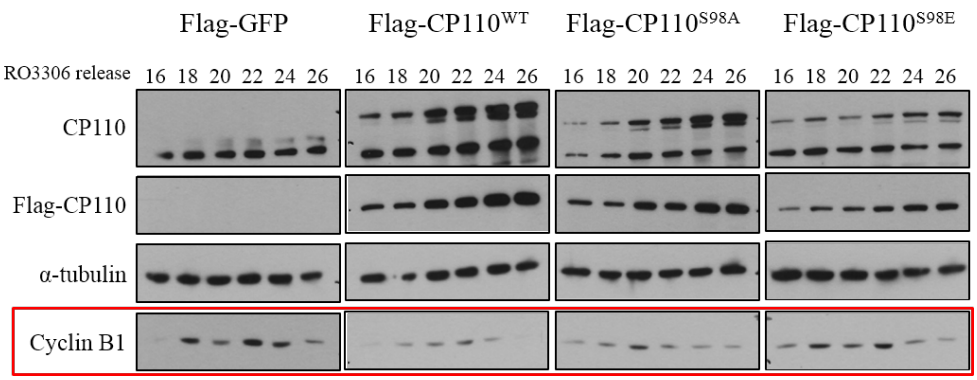
Flag-GFP
Flag-CP110WT
Flag-CP110S98A
Flag-CP110S98E
RO3306 release
16 18 20 22 24 26
16 18 20 22 24 26
16 18 20 22 24 26
16 18 20 22 24 26
CP110
Flag-CP110
α-tubulin
Cyclin B1

**Figure 23. The phospho-mimetic mutant of CP110 rescued the PLK4 knockdown phenotype of centriole duplication.** The Flag-CP110 and Flag-CP110$^{S98E}$ were ectopically expressed in PLK4-depleted cells. Thirty-six hours after the siRNA transfection, the HeLa cells were immunostained with antibodies against centrin2 and Flag. Graph shows percent of cells with 3 or 4 centrin dots. The experiments were repeated 3 times.

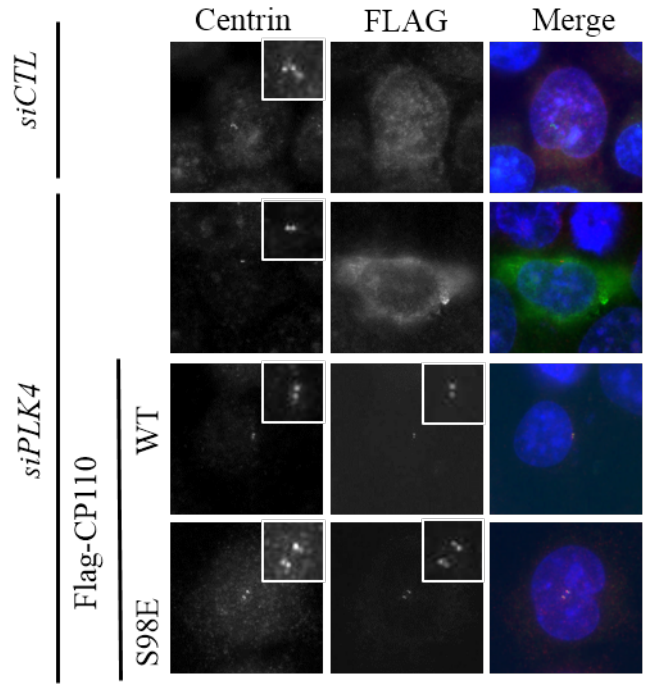
Centrin
FLAG
Merge
siCTL
siPLK4
Flag-CP110
WT
S98E

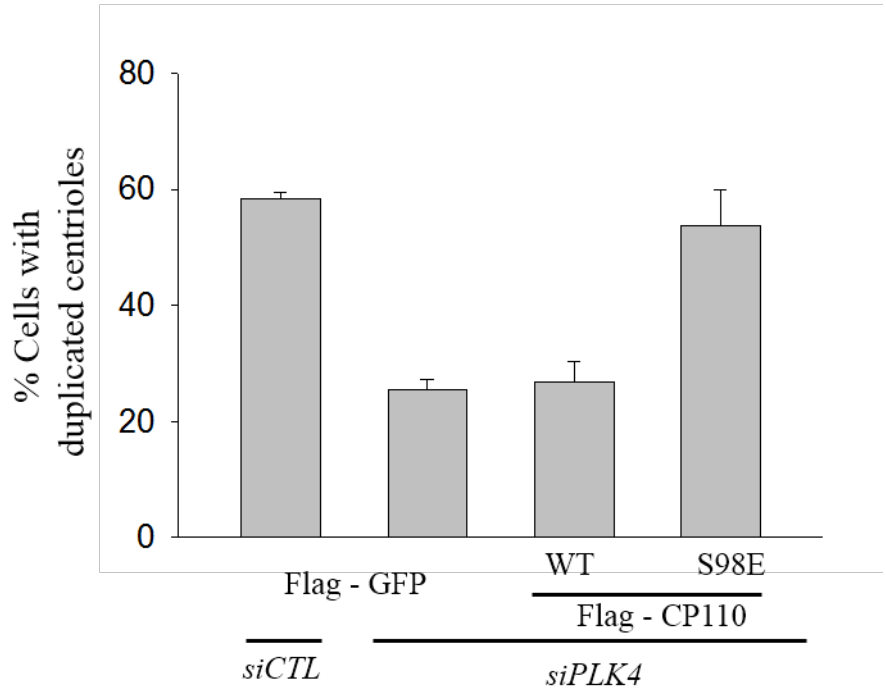
% Cells with duplicated centrioles
80
60
40
20
0
Flag - GFP
WT
S98E
Flag - CP110
siCTL
siPLK4

**Figure 24. The stably expressed phospho-mimetic mutant of CP110 rescued the PLK4 knockdown phenotype of centriole duplication.** (A) Experimental scheme of the knockdown and doxycycline induction in stable cell line. (B) The U2OS TRE/GFP stable line was treated with control and PLK4 siRNAs. Thirty-six hours later, the cells were immunostained with antibodies specific to Flag and centrin. Graph shows the percent of cells with 3 or 4 centrin dots. The experiments were repeated 3 times. (C) PLK4 was depleted in the U2OS cells which stably expressed Flag-CP110, Flag-CP110$^{S98A}$ and Flag-CP110$^{S98E}$. Thirty-six hours after the siRNA transfection, the cells were immunostained with antibodies specific to Flag and centrin. The graph shows the percent of cells with 3 or 4 centrin dots. The experiments were repeated 3 times. Results are presented as means and standard errors. *, $P<0.05$

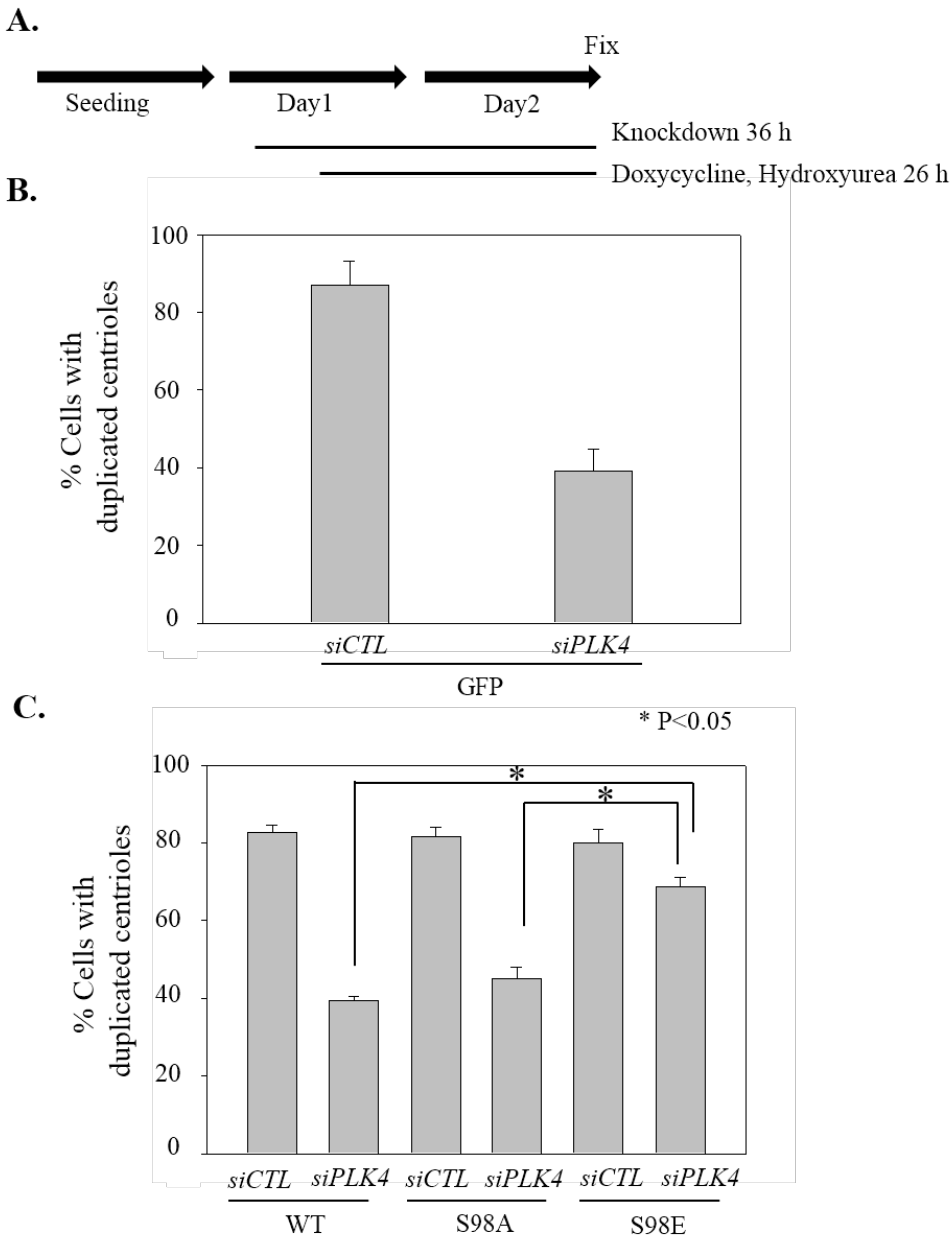
A.
Fix
Seeding
Day1
Day2
Knockdown 36 h
Doxycycline, Hydroxyurea 26 h
B.
% Cells with duplicated centrioles
100
80
60
40
20
0
siCTL
siPLK4
GFP
C.
* P<0.05
% Cells with duplicated centrioles
100
80
60
40
20
0
siCTL
siPLK4
siCTL
siPLK4
siCTL
siPLK4
WT
S98A
S98E

**Figure 25. Detection of procentrioles in the Flag-CP110$^{S98E}$–rescued cells.** PLK4 was depleted in U2OS cells which stably expressed Flag-CP110 and Flag-CP110$^{S98E}$. The cells were immunostained with the antibodies against centrin and centrobin. The graph shows the percent of cells with two or more centrobin dots.

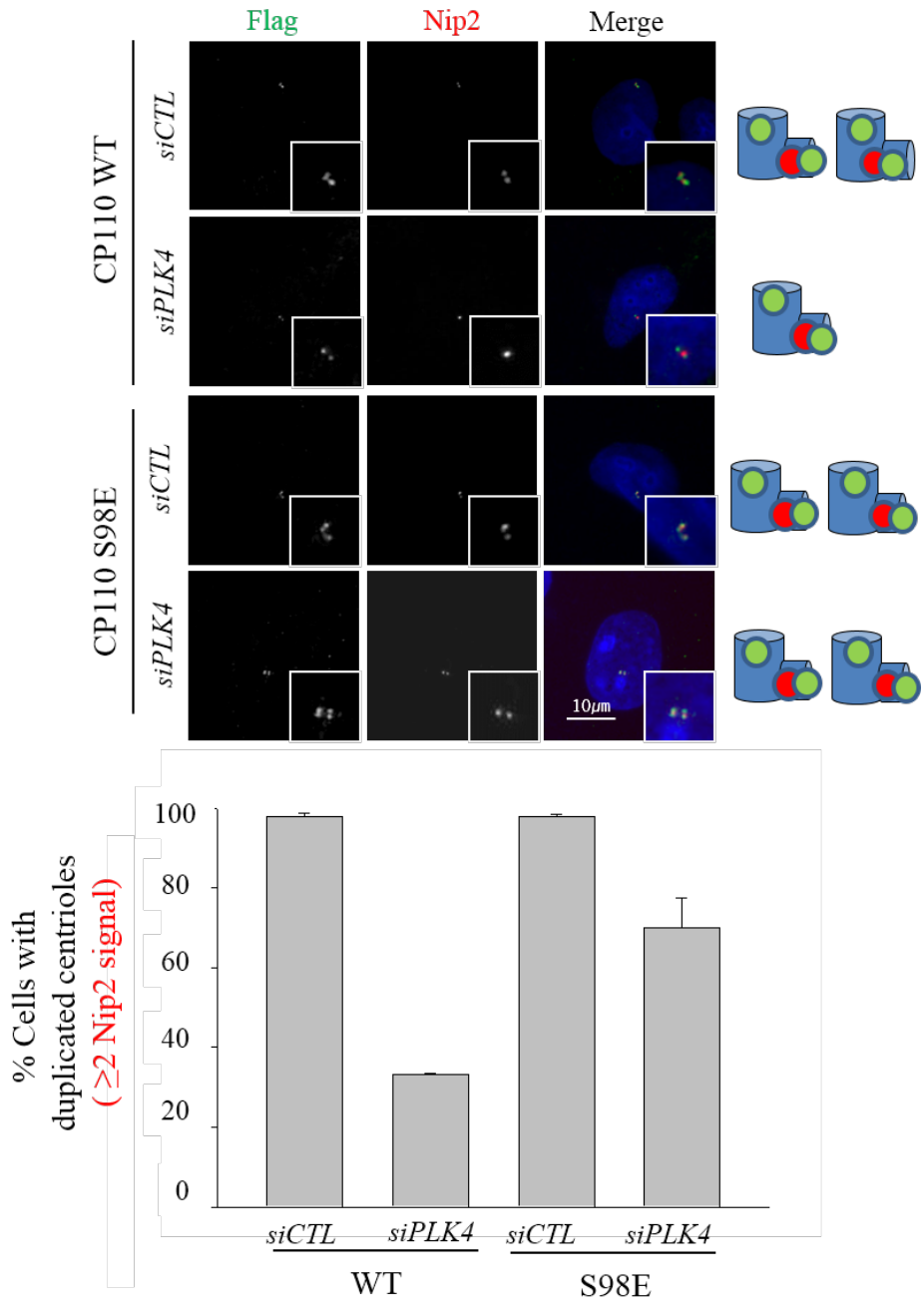
Flag
Nip2
Merge
CP110 WT
siCTL
siPLK4
CP110 S98E
siCTL
siPLK4
10μm
% Cells with duplicated centrioles (≥2 Nip2 signal)
100
80
60
40
20
0
siCTL
siPLK4
siCTL
siPLK4
WT
S98E

**Figure 26. Detection of the centrosomal SAS-6 signals in the Flag-CP110$^{S98E}$–rescued cells.** PLK4 was depleted in U2OS cells which stably expressed Flag-CP110 and Flag-CP110$^{S98E}$. The cells were immunostained with the antibodies against centrin and SAS-6. The graphs show the percent cells with duplicated centrioles with and without SAS-6 signals. Scale bar represents 10 μm. For statistical analysis, over 300 cells were counted per experimental group and the experiments were repeated twice.

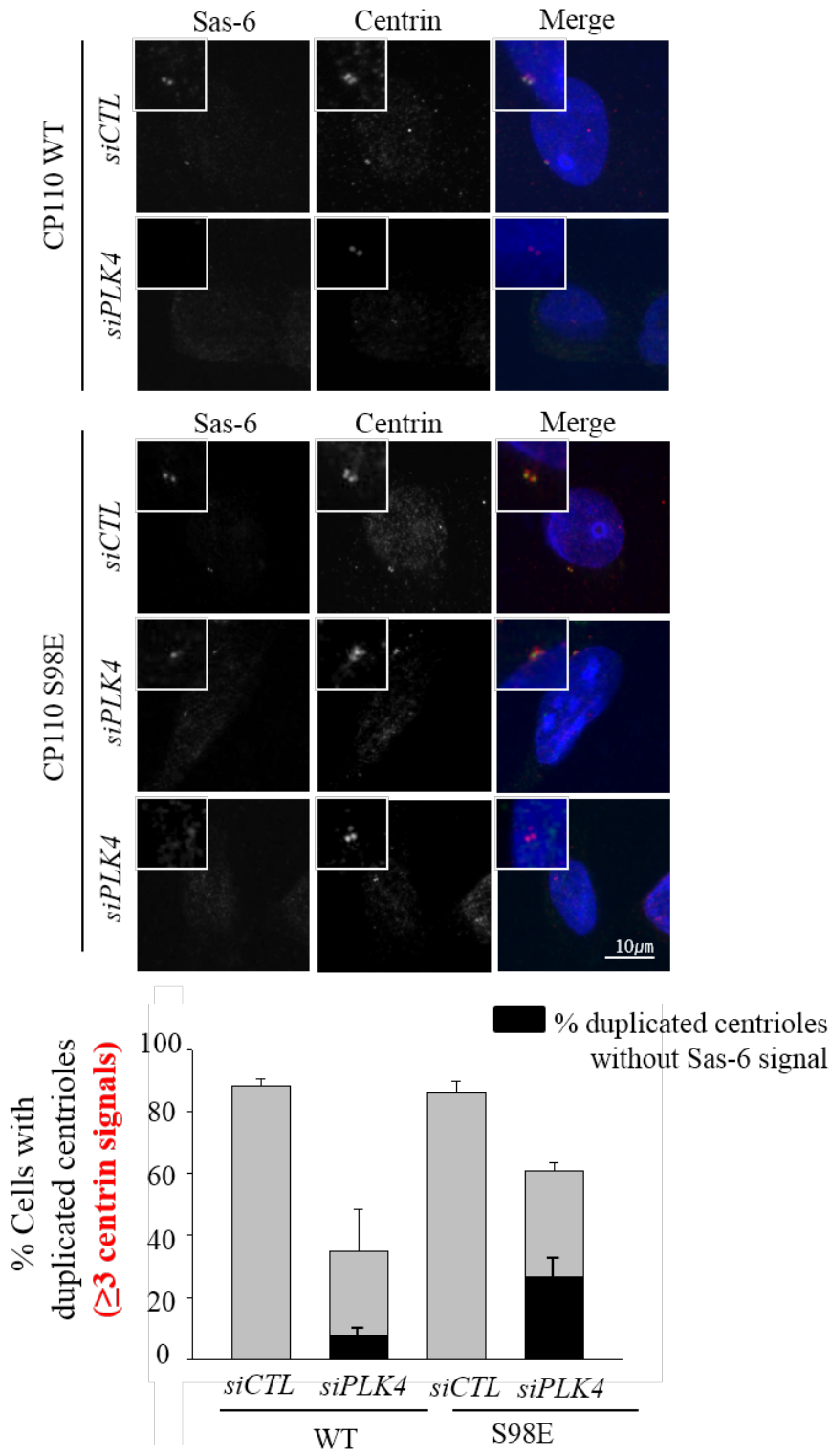
Sas-6
Centrin
Merge
CP110 WT
siCTL
siPLK4
CP110 S98E
siCTL
siPLK4
siPLK4
10µm
% duplicated centrioles without Sas-6 signal
% Cells with duplicated centrioles (≥3 centrin signals)
100
80
60
40
20
0
siCTL
siPLK4
siCTL
siPLK4
WT
S98E

**Figure 27. The phospho-mimetic mutant of CP110 did not rescue the SAS-6 knockdown phenotype of centriole duplication.** (A) Experimental scheme inU2OS stable line. (B) SAS-6 was depleted in the U2OS cells which stably expressed Flag-CP110, Flag-CP110$^{S98A}$ and Flag-CP110$^{S98E}$. Forty-eight hours after the siRNA transfection, the cells were immunostained with antibodies against Flag and centrin. Graph shows the percent of cells with 3 or 4 centrin dots. The experiments were repeated 3 times.

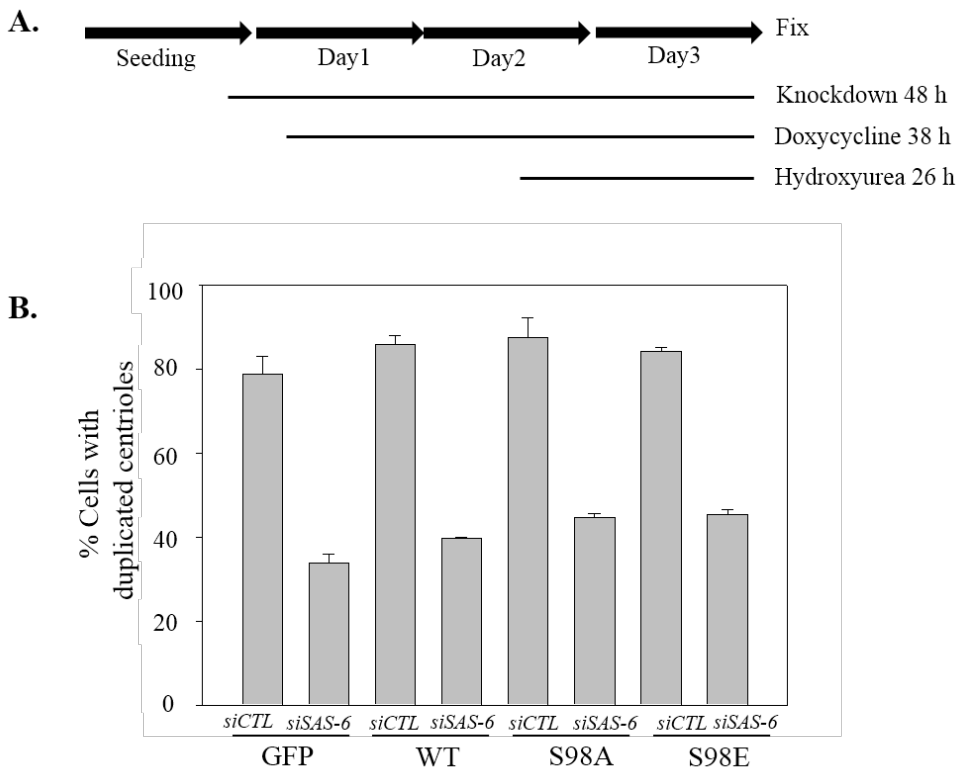
A.
Seeding
Day1
Day2
Day3
Fix
Knockdown 48 h
Doxycycline 38 h
Hydroxyurea 26 h
B.
% Cells with duplicated centrioles
100
80
60
40
20
0
siCTL
siSAS-6
siCTL
siSAS-6
siCTL
siSAS-6
siCTL
siSAS-6
GFP
WT
S98A
S98E

**Figure 28. The phospho-mimetic mutant of CP110 did not rescue the CPAP knockdown phenotype of centriole duplication.** (A) Experimental scheme in U2OS stable line. (B) CPAP was depleted in the U2OS cells which stably expressed Flag-CP110, Flag-CP110$^{S98A}$ and Flag-CP110$^{S98E}$. Forty-eight hours after the siRNA transfection, the cells were immunostained with antibodies against Flag and centrin. Graph shows the percent of cells with 3 or 4 centrin dots. The experiments were repeated 3 times.

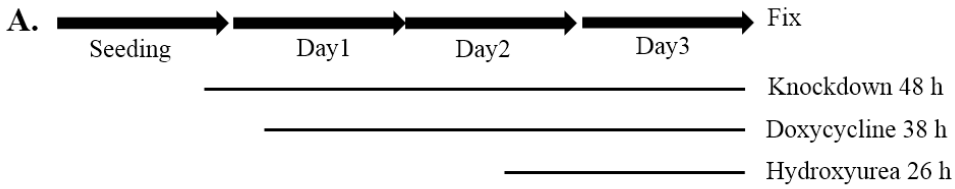
A.
Seeding
Day1
Day2
Day3
Fix
Knockdown 48 h
Doxycycline 38 h
Hydroxyurea 26 h

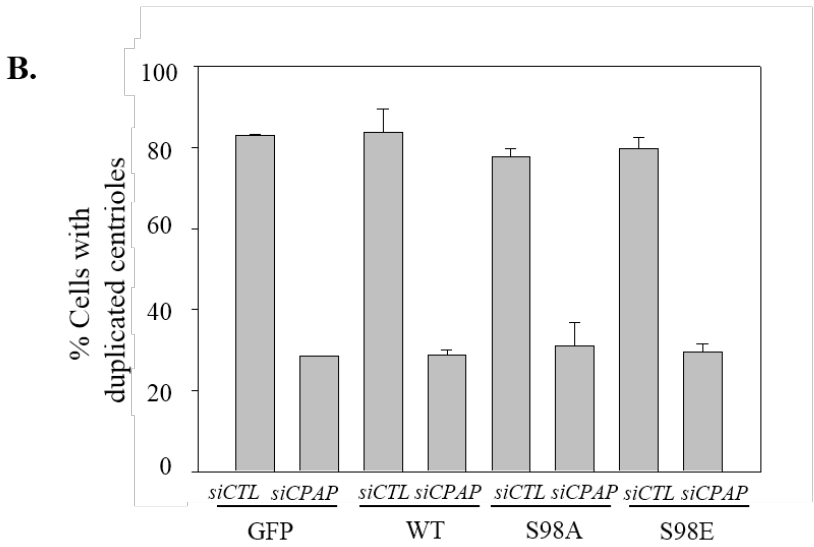
B.
% Cells with duplicated centrioles
100
80
60
40
20
0
siCTL siCPAP siCTL siCPAP siCTL siCPAP siCTL siCPAP
GFP
WT
S98A
S98E

**Figure 29. The cellular CP110 levels during mitosis.** The cell cycle of the HeLa stable lines which expressed Flag-CP110, Flag-CP110$^{S98A}$ and Flag-CP110$^{S98E}$ were synchronized with the double thymidine block and release. STLC was added to block the cell cycle at M phase. At indicated time points, the cells were subjected to immunoblot analysis with antibodies specific to CP110, cyclin B1, $\alpha$-tubulin and phospho-histone H3.

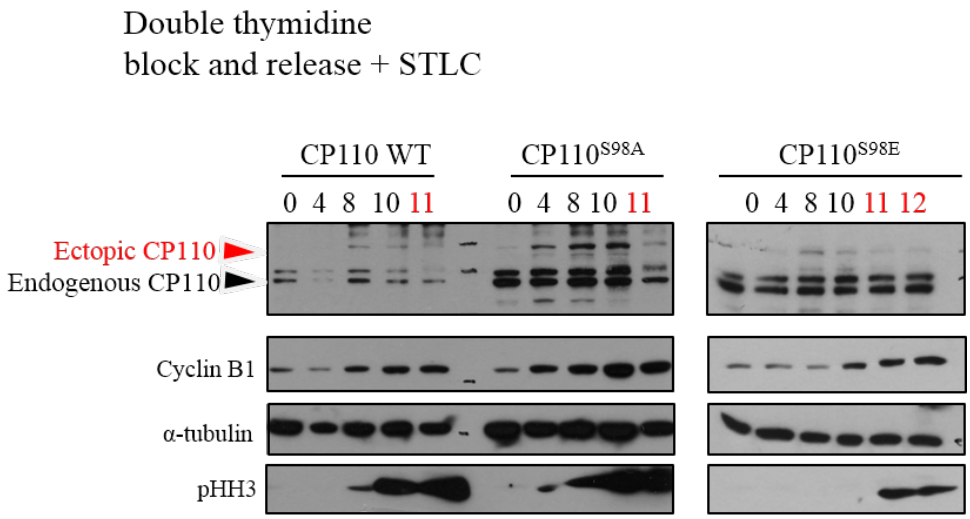
Double thymidine
block and release + STLC
CP110 WT
CP110S98A
CP110S98E
0 4 8 10 11
0 4 8 10 11
0 4 8 10 11 12
Ectopic CP110
Endogenous CP110
Cyclin B1
α-tubulin
pHH3

**Figure 30. The phospho-resistant mutation of CP110 did not affect the interaction with Kif24 and CEP97.** 293T cells were transfected with Flag-CP110 and pFlag-CP110$^{S98A}$. Forty-eight hours later, the cells were subjected to immunoprecipitation with the Kif24 and CEP97 antibodies followed by immunoblot analysis with the Kif24, CEP97 and Flag antibodies.

**A.**

IP : α-Kif24

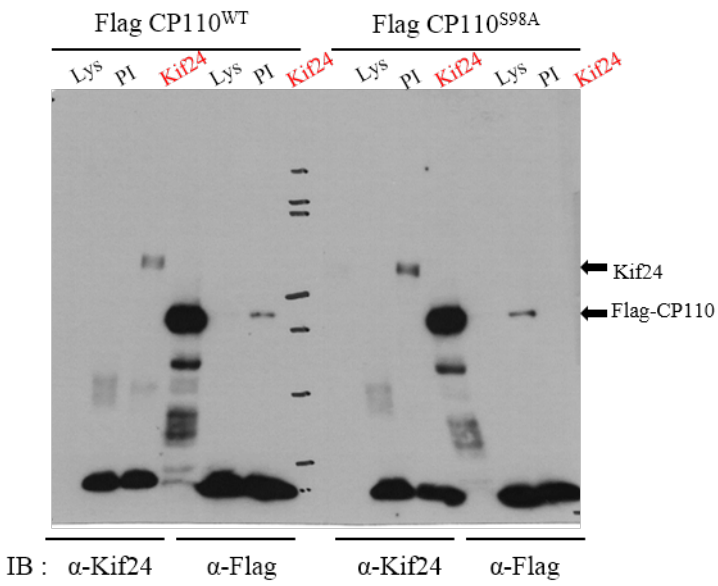


**B.**

IP : α-CEP97

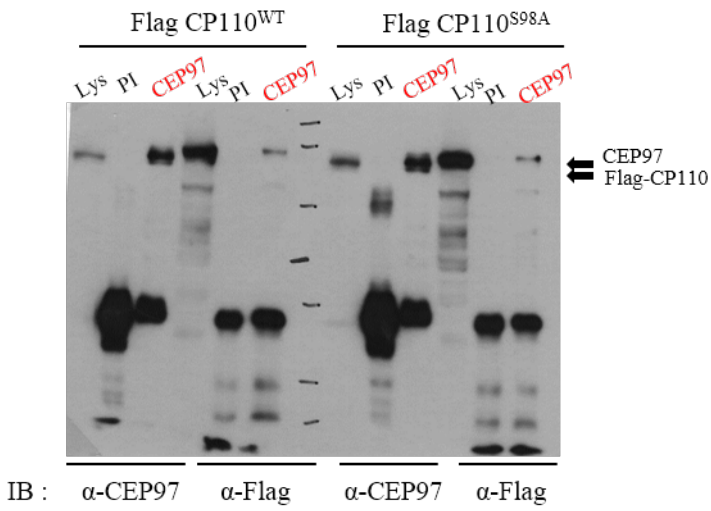

**Figure 31. Centrosomal localization of pCP110$^{S98}$.** (A) HeLa cells were immunostained with antibodies specific to centrin and pCP110$^{S98}$. (B) U2OS cells were immunostained with antibodies specific to centrin and pCP110$^{S98}$. Fixed cells were observed with structural illuminating microscopy (SIM). The right panel is an interpretation of the immunostaining images.

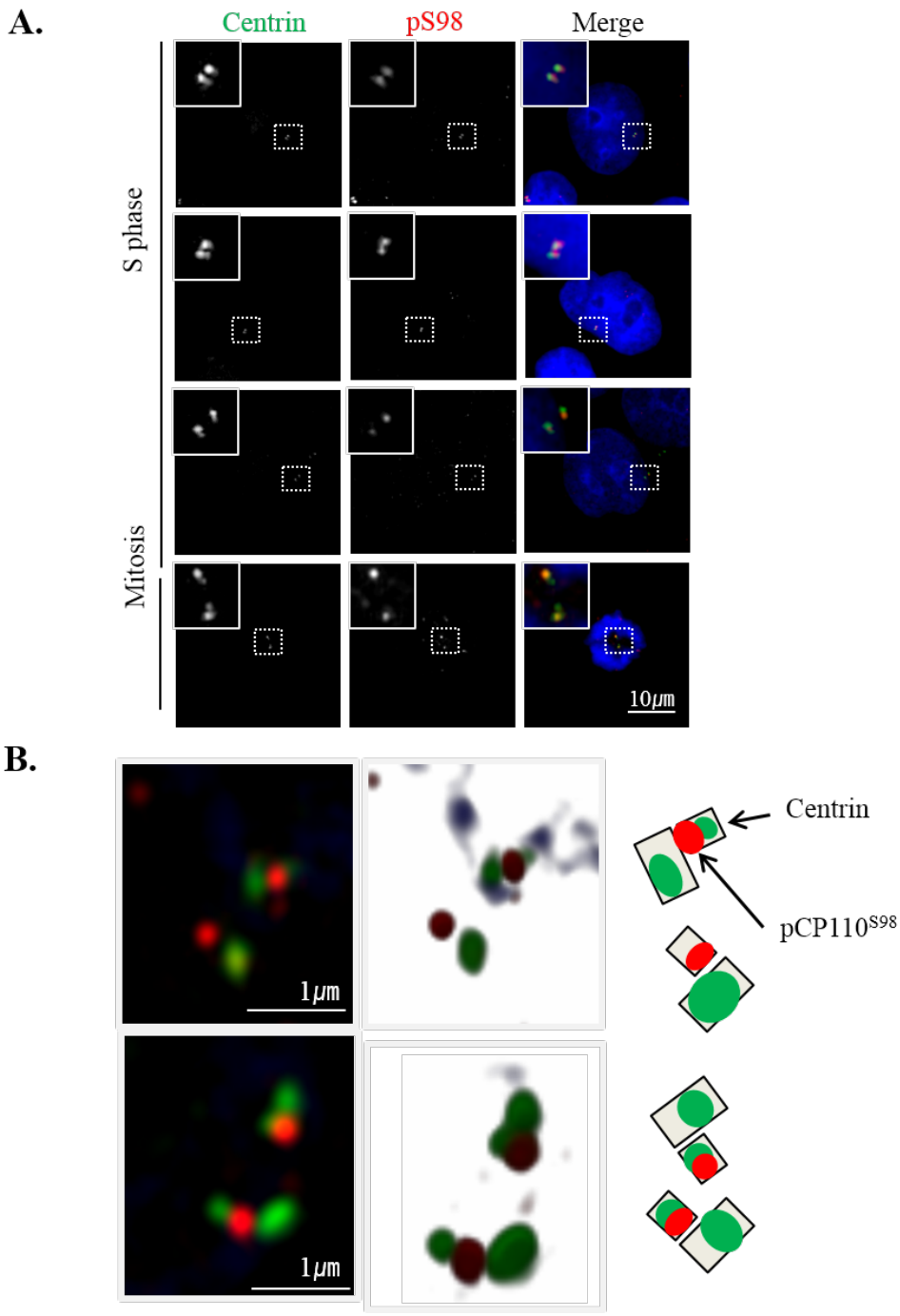
A.
Centrin
pS98
Merge
S phase
Mitosis
10μm
B.
1μm
1μm
Centrin
pCP110S98

**Figure 32. Coimmunostaining of CP110 and pCP110$^{S98}$.** U2OS cells were arrested at G1/S phase with 0.5mM mimosine for 20 hours. Mimosine inhibits DNA replication and arrests the cell cycle in the G1/S phase. The cells were immunostained with antibodies specific to centrin (red), pCP110$^{S98}$ (green) and CP110 (blue). The CP110 antibody was conjugated with Zenon Alexa 488 labeling dye. The mother and procentrioles were outlined with the yellow and blue boxes, respectively.

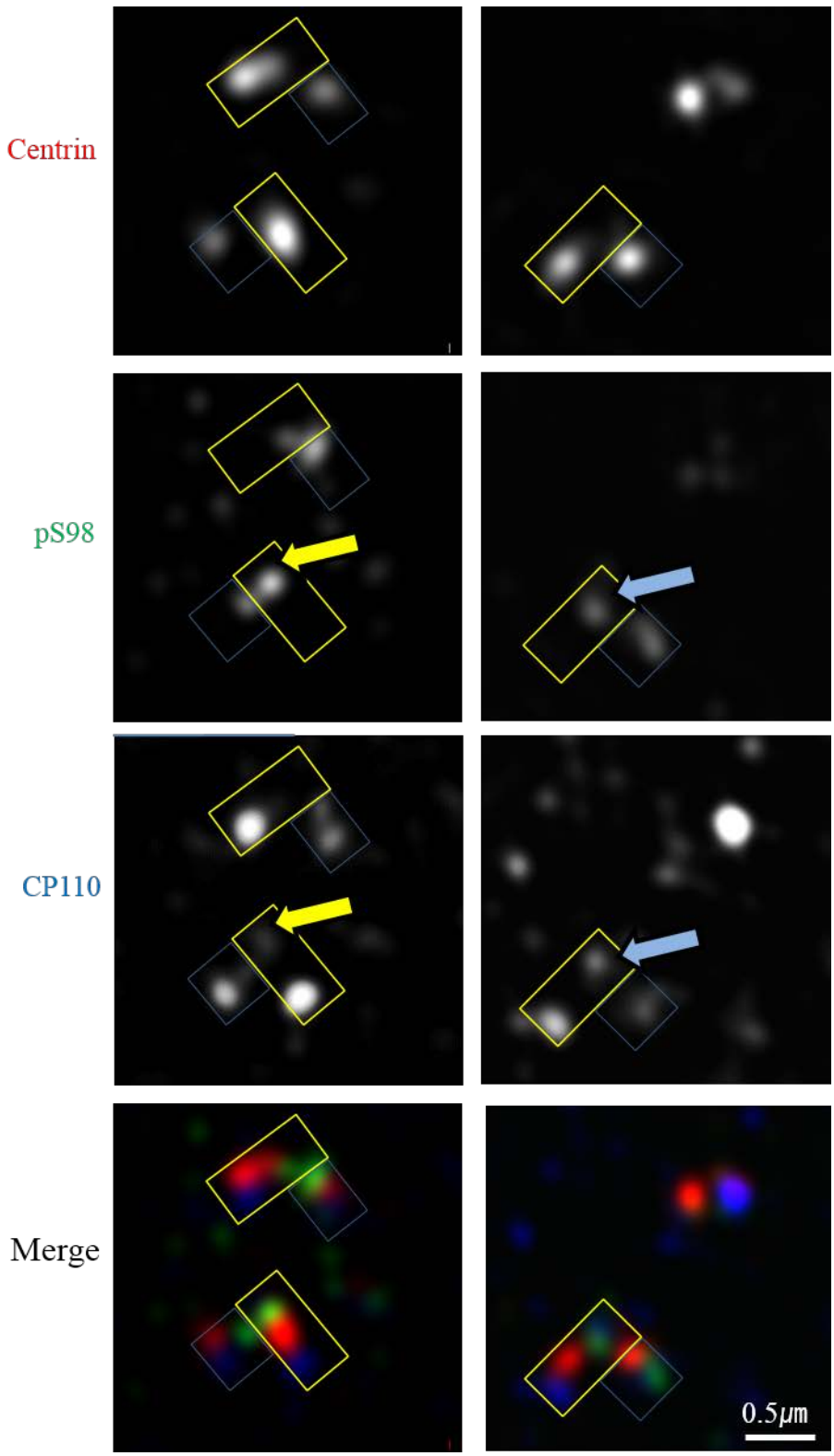
Centrin
pS98
CP110
Merge
0.5μm

**Figure 33. CP110 signals at the proximal ends as well as the distal ends of the centrioles.** HeLa cells at early S phase were immunostained with antibodies specific to centrin and CP110. The mother and procentrioles were outlined with the yellow and blue boxes, respectively.

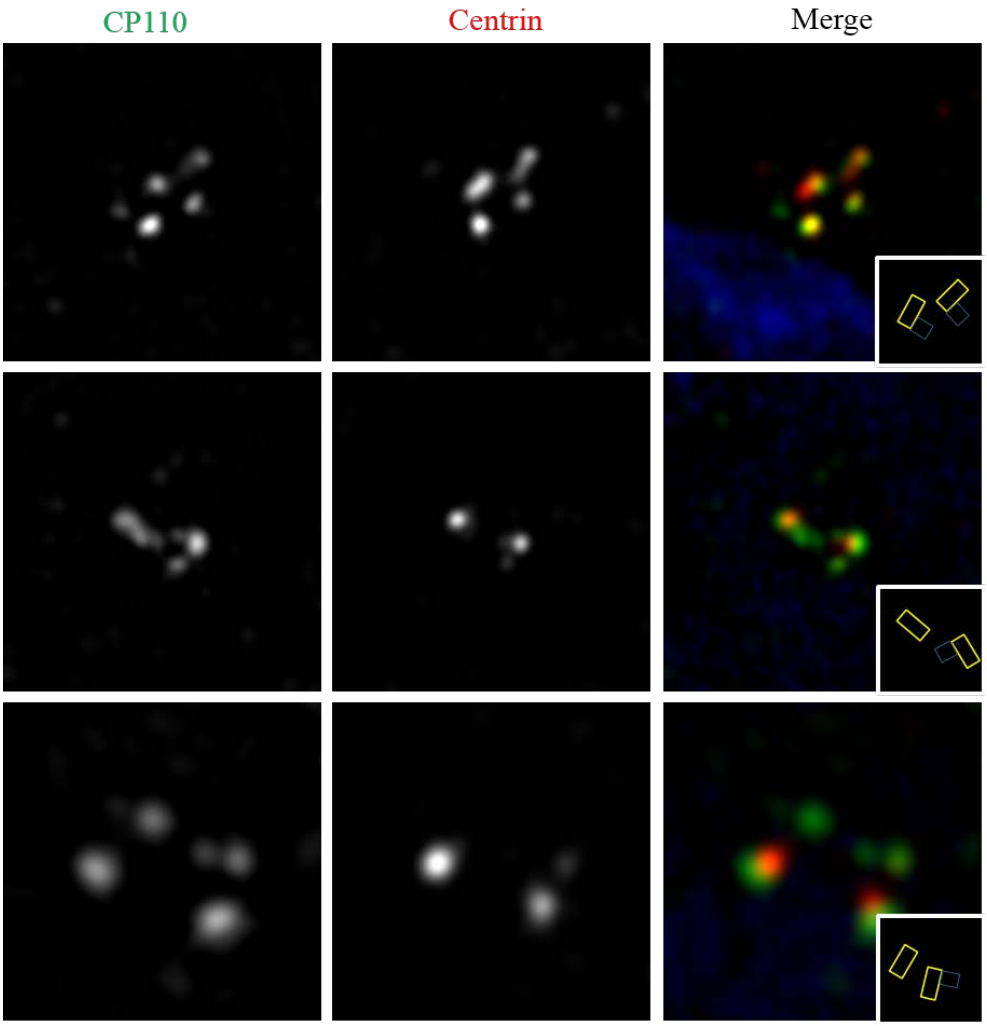
CP110
Centrin
Merge

**Figure 34. CP110 recruitment in centriole assembly.** (A) HeLa cells were fixed at 3(G1), 8(Early S), 14(S) hours after mitotic release. Cells were stained with antibodies specific to centrin and CP110. (B) HeLa cells were fixed 8 h (Early S) after mitotic release. HeLa cells were stained with antibodies specific to CP110 and Sas-6.

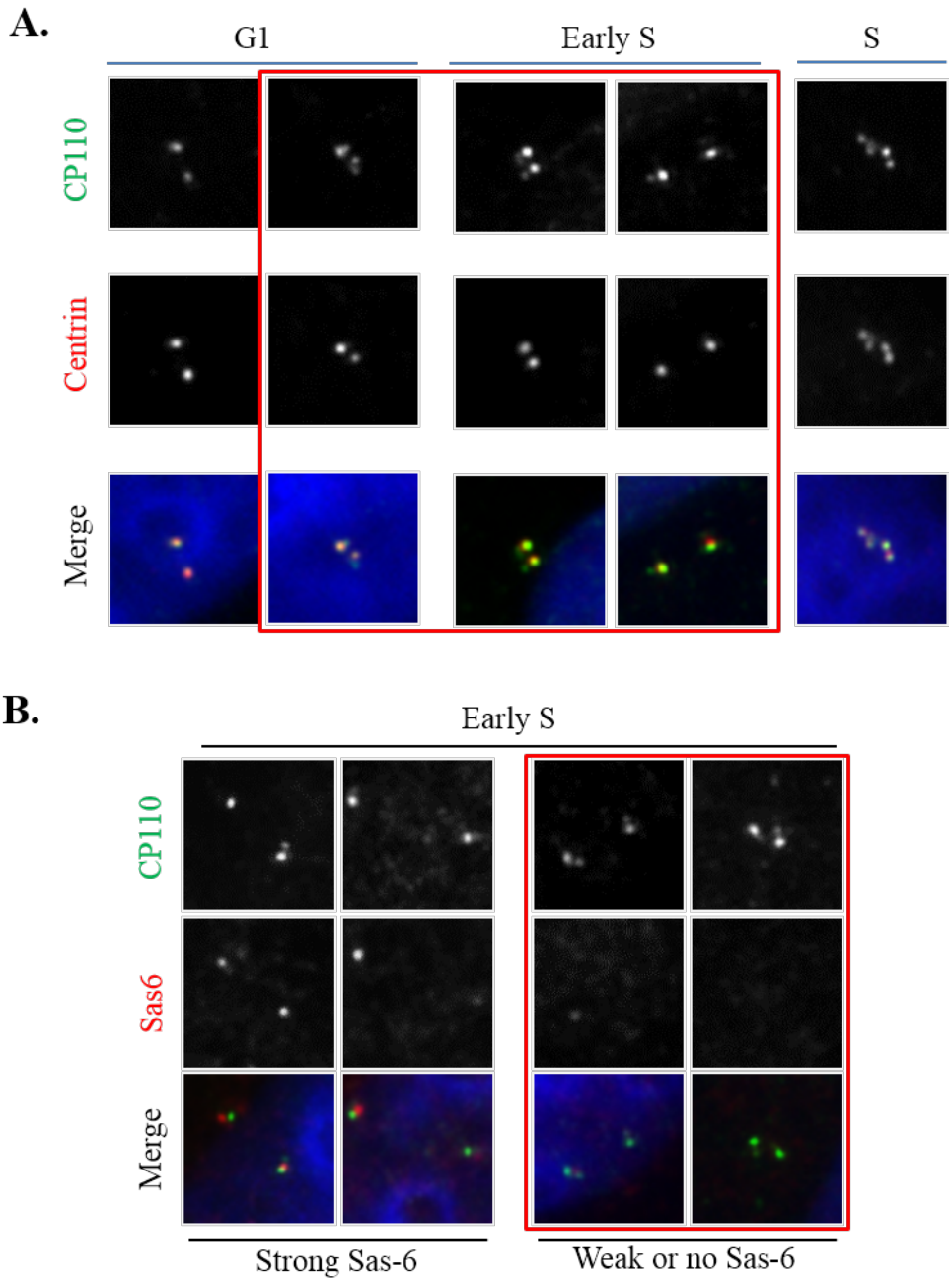
A.
G1
Early S
S
CP110
Centrin
Merge
B.
Early S
CP110
Sas6
Merge
Strong Sas-6
Weak or no Sas-6

**Figure 35. Working model.** CP110 as well as other centriole components are recruited to the site where new procentriole is assembled. PLK4 phosphorylation of CP110 is a critical step for stabilization of the recruited centriole components. The phospho-mimetic CP110 may stabilize available centriole components even in the PLK4-depleted cells.

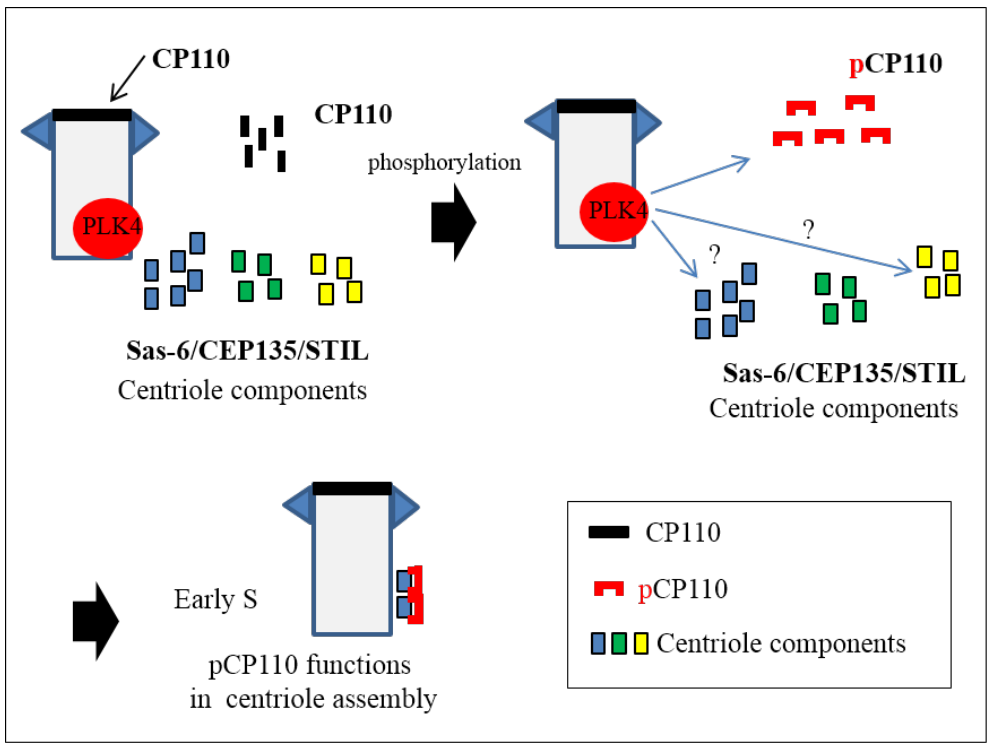
CP110
CP110
phosphorylation
pCP110
PLK4
PLK4
?
?
Sas-6/CEP135/STIL
Centriole components
Sas-6/CEP135/STIL
Centriole components
Early S
pCP110 functions
in centriole assembly
CP110
pCP110
Centriole components

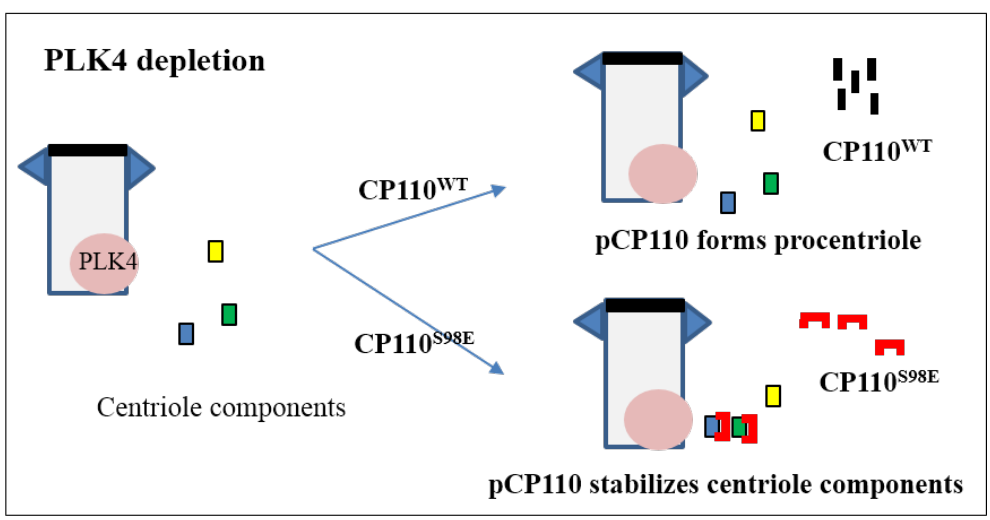
PLK4 depletion
PLK4
CP110WT
CP110S98E
Centriole components
CP110WT
pCP110 forms procentriole
CP110S98E
pCP110 stabilizes centriole components

# Discussion

Studies using the phospho-CP110 specific antibody (pCP110$^{S98}$) revealed that PLK4 phosphorylates the site. The phosphorylation pattern of CP110 correlates with the activity pattern of PLK4 (Cunha-Ferreira, 2009; Rogers, 2009). However, the precise biological function of PLK4 during mitosis is still unclear, even if the PLK4 activity is the highest at M phase. Rather, it is though that PLK4 might be critical for initiation of centriole assembly at early S phase. Similarly, phosphorylation of CP110 was regulated in a cell cycle stage-specific manner, reaching a maximal level at M phase and diminishing to a basal level after the mitotic exit. Therefore, phospho-CP110 may also be involved in centriole assembly in early S phase despite the moderate phosphorylation level of CP110.

The rescue experiments revealed the importance of phosphorylation at serine 98 residue of CP110 in centriole assembly. The phospho-resistant mutant of CP110 blocked centriole overduplication in S phase-arrested cells while the phospho-mimetic mutant of CP110 enhanced centriole assembly in PLK4-depleted cells. These results support the notion that specific phosphorylation of CP110 is essential for centriole assembly. Despite the importance of CP110 phosphorylation in centriole assembly, we did not observe decrease in duplication using phospho-resistant mutant stable cell line nor increase in duplication using phospho-mimetic mutant stable cell line. One possible explanation for this is the narrow window of time between doxycycline treatment and cell fixation to observe the change in duplication. In the case of phospho-resistant mutant of CP110 stable cell line, it might need more time to replace

endogenous CP110. CP110 is too stable to be completely depleted even in 72 h knockdown period in order to observe significant centriole reduction. In this situation, it is hard to expect that the phospho-resistant mutant of CP110 suppresses centriole assembly.

It is of interest that the $CP110^{S98E}$ can rescue the PLK4 depletion since PLK4 is considered an initiator of the centriole assembly. However, $CP110^{S98E}$ did not rescue centriole assembly in SAS6- and CPAP-depleted cells, suggesting that phosphorylation of CP110 is an upstream event of the cartwheel formation and centriole elongation. My results propose that CP110 is a key substrate of PLK4 for centriole assembly and that phosphorylation of CP110 might be sufficient for PLK4 function in centriole assembly. Based on these results, we propose a model that the phospho-CP110 plays a role in assembling components for procentrioles (Figure 38). Localization of PLK4 at the assembly site may be the initial step. CP110 is phosphorylated by PLK4 at the site, which helps to stabilize and assemble procentriole components. Even without PLK4, the phospho-mimetic mutant of CP110 may still stabilize the components at the site for procentriole assembly (Figure 38). In support of the hypothesis, $CP110^{S98E}$ still enhanced procentriole assembly even with a reduced amount of SAS6 (Figure 31).

CP110 is localized at the distal end of centriole and functions as a capping protein. CP110 should be removed from the centriole when cilia is formed (Spektor, 2007; Tsang, 2008). In my observation, $pCP110^{S98}$ is not detected at the distal end of mother centriole. Therefore, it is not sure whether phosphorylation of CP110 is involved in cilia formation or not. Instead, I observed additional CP110 signal at the

proximal part of daughter centriole, and this signal co-localized with pCP110 signal. These localizations of CP110 and pCP110$^{S98}$ support the notion that CP110 is essential for procentriole assembly in early S phase.

# References


Arquint, C., and Nigg, E.A. (2014). STIL microcephaly mutations interfere with APC/C-mediated degradation and cause centriole amplification. Curr Biol *24*, 351-360.

Azimzadeh, J., Marshall, W.F. (2010). Building the centriole. Curr Biol *20*, 816-825.

Bahtz, R., Seidler, J., Arnold, M., Haselmann-Weiss, U., Antony, C., Lehmann, W.D., and Hoffmann, I. (2012). GCP6 is a substrate of Plk4 and required for centriole duplication. J Cell Sci *125*, 486-496.

Bettencourt-Dias, M., Rodrigues-Martins, A., Carpenter, L., Riparbelli, M., Lehmann, L., Gatt, M.K., Carmo, N., Balloux, F., Callaini, G., and Glover, D.M. (2005). SAK/PLK4 is required for centriole duplication and flagella development. Curr Biol *15*, 2199-2207.

Bond, J., Roberts, E., Springell, K., Lizarraga, S.B., Scott, S., Higgins, J., Hampshire, D.J., Morrison, E.E., Leal, G.F., Silva, E.O., *et al.* (2005). A centrosomal mechanism involving CDK5RAP2 and CENPJ controls brain size. Nat Genet *37*, 353-355.

Bornens, M., Paintrand, M., Berges, J., Marty, M.C., and Karsenti, E. (1987). Structural and chemical characterization of isolated centrosomes. Cell Motil Cytoskeleton 8, 238-249.

Bouckson-Castaing, V., Moudjou, M., Ferguson, D.J., Mucklow, S., Belkaid, Y., Milon, G., Crocker, P.R. (1996). Molecular characterisation of ninein, a new coiled-coil protein of thecentrosome. J Cell Sci *109*,179-190.

Brownlee, C.W., Klebba, J.E., Buster, D.W., and Rogers, G.C. (2011). The Protein Phosphatase 2A regulatory subunit Twins stabilizes Plk4 to induce centriole amplification. J Cell Biol *195*, 231-243.

Cajanek, L., and Nigg, E.A. (2014). Cep164 triggers ciliogenesis by recruiting Tau tubulin kinase 2 to the mother centriole. . Proc Natl Acad Sci U S A *111*, E2841-2850.

Carvalho-Santos, Z., Machado, P., Branco, P., Tavares-Cadete, F., Rodrigues-Martins, A., Pereira-Leal, J.B., and Bettencourt-Dias, M. (2010). Stepwise evolution of the centriole-assembly pathway. J Cell Sci *123*, 1414-1426.

Chang, J., Cizmecioglu, O., Hoffmann, I., and Rhee, K. (2010). PLK2 phosphorylation is critical for CPAP function in procentriole formation during the centrosome cycle. EMBO J *29*, 2395-2406.

Chavali, P.L., Putz, M., and Gergely, F. (2014). Small organelle, big responsibility: the

role of centrosomes in development and disease. Philos Trans R Soc Lond B Biol Sci *369*.

Chen, Z., Indjeian, V.B., McManus, M., Wang, L., and Dynlacht, B.D. (2002). CP110, a cell cycle-dependent CDK substrate, regulates centrosome duplication in human cells. Dev Cell *3*, 339-350.

Comartin, D., Gupta, G.D., Fussner, E., Coyaud, E., Hasegan, M., Archinti, M., Cheung, S.W., Pinchev, D., Lawo, S., Raught, B., *et al.* (2013). CEP120 and SPICE1 cooperate with CPAP in centriole elongation. Curr Biol *23*, 1360-1366.

Cottee, M.A., Raff, J.W., Lea, S.M., and Roque, H. (2011). SAS-6 oligomerization: the key to the centriole? Nat Chem Biol *7*, 650-653.

Cunha-Ferreira I., Rodrigues-Martins A., Bento I., Riparbelli M., Zhang W., Laue E., Callaini G., Glover D.M., Bettencourt-Dias M. (2009). The SCF/Slimb ubiquitin ligase limits centrosome amplification through degradation of SAK/PLK4. Curr Biol *19*, 43-49.

D'Angiolella, V., Donato, V., Vijayakumar, S., Saraf, A., Florens, L., Washburn, M.P., Dynlacht, B., and Pagano, M. (2010). SCF (Cyclin F) controls centrosome homeostasis and mitotic fidelity through CP110 degradation. Nature *466*, 138-142.

Dammermann, A., Maddox, P.S., Desai, A., and Oegema, K. (2008). SAS-4 is recruited to a dynamic structure in newly forming centrioles that is stabilized by the gamma-tubulin-mediated addition of centriolar microtubules. J Cell Biol *180*, 771-785.

Desai, A., and Mitchison, T.J. (1997). Microtubule polymerization dynamics. Annu Rev Cell Dev Biol *13*, 83-117.

Duensing, A., Liu, Y., Tseng, M., Malumbres, M., Barbacid, M., and Duensing, S. (2006). Cyclin-dependent kinase 2 is dispensable for normal centrosome duplication but required for oncogene-induced centrosome overduplication. Oncogene *25*, 2943-2949.

Dylewski, D.P., and Keenan, T.W. (1984). Centrioles in the mammary epithelium of the rat. J Cell Sci *72*, 185-193.

Fry, A.M., Mayor, T., Meraldi, P., Stierhof, Y.D., Tanaka, K., and Nigg, E.A. (1998). C-Nap1, a novel centrosomal coiled-coil protein and candidate substrate of the cell cycle-regulated protein kinase Nek2. J Cell biol *141*, 1563-1574.

Fu, J., and Glover, D.M. (2012). Structured illumination of the interface between centriole and peri-centriolar material. Open Biol *2*, 120104.

Gillies, T.E., and Cabernard, C. (2011). Cell division orientation in animals. Curr Biol *21*, R599-609.

Gonczy, P. (2012). Towards a molecular architecture of centriole assembly. Nat Rev Mol Cell Biol *13*, 425-435.

Gopalakrishnan, J., Mennella, V., Blachon, S., Zhai, B., Smith, A.H., Megraw, T.L., Nicastro, D., Gygi, S.P., Agard, D.A., and Avidor-Reiss, T. (2011). Sas-4 provides a scaffold for cytoplasmic complexes and tethers them in a centrosome. Nat Commun *2*, 359.

Guderian, G., Westendorf, J., Uldschmid, A., and Nigg, E.A. (2010). Plk4 trans-autophosphorylation regulates centriole number by controlling betaTrCP-mediated degradation. J Cell Sci *123*, 2163-2169.

Gudi, R., Zou, C., Li, J., and Gao, Q. (2011). Centrobin-tubulin interaction is required for centriole elongation and stability. J Cell Biol *193*, 711-725.

Guichard, P., Chretien, D., Marco, S., and Tassin, A.M. (2010). Procentriole assembly revealed by cryo-electron tomography. EMBO J *29*, 1565-1572.

Habedanck, R., Stierhof, Y.D., Wilkinson, C.J., and Nigg, E.A. (2005). The Polo kinase Plk4 functions in centriole duplication. Nat Cell Biol *7*, 1140-1146.

Hatch, E.M., Kulukian, A., Holland, A.J., Cleveland, D.W., and Stearns, T. (2010). Cep152 interacts with Plk4 and is required for centriole duplication. J Cell Biol *191*, 721-729.

He, R., Huang, N., Bao, Y., Zhou, H., Teng, J., and Chen, J. (2013). LRRC45 is a centrosome linker component required for centrosome cohesion. Cell reports *4*, 1100-1107.

Hinchcliffe, E.H., Li, C., Thompson, E.A., Maller, J.L., and Sluder, G. (1999). Requirement of Cdk2-cyclin E activity for repeated centrosome reproduction in Xenopus egg extracts. Science *283*, 851-854.

Hirono, M. (2014). Cartwheel assembly. Philos Trands R Soc Lond B Biol Sci *369*.

Hodges, M.E., Scheumann, N., Wickstead, B., Langdale, J.A., and Gull, K. (2010). Reconstructing the evolutionary history of the centriole from protein components. J Cell Sci *123*, 1407-1413.

Holland, A.J., Fachinetti, D., Zhu, Q., Bauer, M., Verma, I.M., Nigg, E.A., and Cleveland, D.W. (2012). The autoregulated instability of Polo-like kinase 4 limits centrosome duplication to once per cell cycle. Genes & Dev *26*, 2684-2689.

Holland, A.J., Lan, W., Niessen, S., Hoover, H., and Cleveland, D.W. (2010). Polo-like kinase 4 kinase activity limits centrosome overduplication by autoregulating its own stability. J Cell Biol *188*, 191-198.

Hsu, L.C., Kapali, M., DeLoia, J.A., and Gallion, H.H. (2005). Centrosome abnormalities in ovarian cancer. Int J Cancer*113*, 746-751.

Ibrahim, R., Messaoudi, C., Chichon, F.J., Celati, C., and Marco, S. (2009). Electron tomography study of isolated human centrioles. Microsc Res Tech *72*, 42-48.

Jana, S.C., Marteil, G., and Bettencourt-Dias, M. (2014). Mapping molecules to structure: unveiling secrets of centriole and cilia assembly with near-atomic resolution. Curr Opin Cell Biol *26*, 96-106.

Keating, T.J., and Borisy, G.G. (1999). Centrosomal and non-centrosomal microtubules. Biol Cell *91*, 321-329.

Keller, D., Orpinell, M., Olivier, N., Wachsmuth, M., Mahen, R., Wyss, R., Hachet, V., Ellenberg, J., Manley, S., and Gonczy, P. (2014). Mechanisms of HsSAS-6 assembly promoting centriole formation in human cells. J Cell Biol *204*, 697-712.

Kim, K., Lee, S., Chang, J., and Rhee, K. (2008). A novel function of CEP135 as a platform protein of C-NAP1 for its centriolar localization. Exp Cell Res *314*, 3692-3700.

Kim, T.S., Park, J.E., Shukla, A., Choi, S., Murugan, R.N., Lee, J.H., Ahn, M., Rhee, K., Bang, J.K., Kim, B.Y., *et al.* (2013). Hierarchical recruitment of Plk4 and regulation of centriole biogenesis by two centrosomal scaffolds, Cep192 and Cep152. Proce Natl Acad Sci U S A *110*, E4849-4857.

Kirkham, M., Muller-Reichert, T., Oegema, K., Grill, S., and Hyman, A.A. (2003). SAS-4 is a C. elegans centriolar protein that controls centrosome size. Cell *112*, 575-587.

Kitagawa, D., Kohlmaier, G., Keller, D., Strnad, P., Balestra, F.R., Fluckiger, I., and Gonczy, P. (2011). Spindle positioning in human cells relies on proper centriole formation and on the microcephaly proteins CPAP and STIL. J Cell Sci *124*, 3884-3893.

Kleylein-Sohn, J., Westendorf, J., Le Clech, M., Habedanck, R., Stierhof, Y.D., and Nigg, E.A. (2007). Plk4-induced centriole biogenesis in human cells. Dev Cell *13*, 190-202.

Kobayashi, T., Tsang, W.Y., Li, J., Lane, W., and Dynlacht, B.D. (2011). Centriolar kinesin Kif24 interacts with CP110 to remodel microtubules and regulate ciliogenesis. Cell *145*, 914-925.

Kodani, A., Salome Sirerol-Piquer, M., Seol, A., Garcia-Verdugo, J.M., and Reiter, J.F. (2013). Kif3a interacts with Dynactin subunit p150 Glued to organize centriole subdistal appendages. EMBO J *32*, 597-607.

Kohlmaier, G., Loncarek, J., Meng, X., McEwen, B.F., Mogensen, M.M., Spektor, A., Dynlacht, B.D., Khodjakov, A., and Gonczy, P. (2009). Overly long centrioles and defective cell division upon excess of the SAS-4-related protein CPAP. Curr Biol *19*, 1012-1018.

Kumar, A., Girimaji, S.C., Duvvari, M.R., and Blanton, S.H. (2009). Mutations in STIL, encoding a pericentriolar and centrosomal protein, cause primary microcephaly. Am J Hum Genet *84*, 286-290.

Kwon, M., Godinho, S.A., Chandhok, N.S., Ganem, N.J., Azioune, A., Thery, M., and Pellman, D. (2008). Mechanisms to suppress multipolar divisions in cancer cells with extra centrosomes. Genes & Dev *22*, 2189-2203.

Lee, K., and Rhee, K. (2012). Separase-dependent cleavage of pericentrin B is necessary and sufficient for centriole disengagement during mitosis. Cell cycle *11*, 2476-2485.

Leidel, S., and Gonczy, P. (2003). SAS-4 is essential for centrosome duplication in C elegans and is recruited to daughter centrioles once per cell cycle. Dev Cell *4*, 431-439.

Lettman, M.M., Wong, Y.L., Viscardi, V., Niessen, S., Chen, S.H., Shiau, A.K., Zhou, H., Desai, A., and Oegema, K. (2013). Direct binding of SAS-6 to ZYG-1 recruits SAS-6 to the mother centriole for cartwheel assembly. Dev Cell *25*, 284-298.

Lin, C.C., Cheng, T.S., Hsu, C.M., Wu, C.H., Chang, L.S., Shen, Z.S., Yeh, H.M., Chang, L.K., Howng, S.L., and Hong, Y.R. (2006). Characterization and functional aspects of human ninein isoforms that regulated by centrosomal targeting signals and evidence for docking sites to direct gamma-tubulin. Cell cycle *5*, 2517-2527.

Lin, Y.N., Wu, C.T., Lin, Y.C., Hsu, W.B., Tang, C.J., Chang, C.W., and Tang, T.K. (2013). CEP120 interacts with CPAP and positively regulates centriole elongation. J Cell Biol *202*, 211-219.

Lingle, W.L., Lutz, W.H., Ingle, J.N., Maihle, N.J., and Salisbury, J.L. (1998). Centrosome hypertrophy in human breast tumors: implications for genomic stability and cell polarity. Proc Natl Acad Sci U S A *95*, 2950-2955.

Loncarek, J., and Khodjakov, A. (2009). Ab ovo or de novo? Mechanisms of centriole duplication. Mol Cells *27*, 135-142.

Matsuo, K., Ohsumi, K., Iwabuchi, M., Kawamata, T., Ono, Y., and Takahashi, M. (2012). Kendrin is a novel substrate for separase involved in the licensing of centriole duplication. Curr Biol *22*, 915-921.

Mennella, V., Keszthelyi, B., McDonald, K.L., Chhun, B., Kan, F., Rogers, G.C., Huang, B., and Agard, D.A. (2012). Subdiffraction-resolution fluorescence

microscopy reveals a domain of the centrosome critical for pericentriolar material organization. Nat Cell Biol *14*, 1159-1168.

Meraldi, P., Lukas, J., Fry, A.M., Bartek, J., and Nigg, E.A. (1999). Centrosome duplication in mammalian somatic cells requires E2F and Cdk2-cyclin A. Nat Cell Biol *1*, 88-93.

Mogensen, M.M., Malik, A., Piel, M., Bouckson-Castaing, V., Bornens, M. (2000). Microtubule minus-end anchorage at centrosomal and non-centrosomal sites: The role of ninein. J Cell Sci *113*,3013-3023.

Moudjou, M., Bordes, N., Paintrand, M., and Bornens, M. (1996). gamma-Tubulin in mammalian cells: the centrosomal and the cytosolic forms. J Cell Sci *109 ( Pt 4)*, 875-887.

Nigg, E.A. (2006). Origins and consequences of centrosome aberrations in human cancers. Int J Cancer *119*, 2717-2723.

Nigg, E.A. (2007). Centrosome duplication: of rules and licenses. Trends Cell Biol *17*, 215-221.

Nigg, E.A., and Stearns, T. (2011). The centrosome cycle: Centriole biogenesis, duplication and inherent asymmetries. Nat Cell Biol *13*, 1154-1160.

Novorol, C., Burkhardt, J., Wood, K.J., Iqbal, A., Roque, C., Coutts, N., Almeida, A.D., He, J., Wilkinson, C.J., and Harris, W.A. (2013). Microcephaly models in the developing zebrafish retinal neuroepithelium point to an underlying defect in metaphase progression. Open Biol *3*, 130065.

O'Connell, K.F., Caron, C., Kopish, K.R., Hurd, D.D., Kemphues, K.J., Li, Y., and White, J.G. (2001). The C. elegans zyg-1 gene encodes a regulator of centrosome duplication with distinct maternal and paternal roles in the embryo. Cell *105*, 547-558.

Ohta, M., Ashikawa, T., Nozaki, Y., Kozuka-Hata, H., Goto, H., Inagaki, M., Oyama, M., and Kitagawa, D. (2014). Direct interaction of Plk4 with STIL ensures formation of a single procentriole per parental centriole. Nat commun *5*, 5267.

Ou, Y.Y., Mack, G.J., Zhang, M., and Rattner, J.B. (2002). CEP110 and ninein are located in a specific domain of the centrosome associated with centrosome maturation. J Cell Sci *115*, 1825-1835.

Paintrand, M., Moudjou, M., Delacroix, H., and Bornens, M. (1992). Centrosome organization and centriole architecture: their sensitivity to divalent cations. J Struct Biol *108*, 107-128.

Palazzo, R.E., Vogel, J.M., Schnackenberg, B.J., Hull, D.R., and Wu, X. (2000). Centrosome maturation. Curr Top Dev Biol *49*, 449-470.

Pelletier, L., O'Toole, E., Schwager, A., Hyman, A.A., and Muller-Reichert, T. (2006). Centriole assembly in Caenorhabditis elegans. Nature *444*, 619-623.

Puklowski, A., Homsi, Y., Keller, D., May, M., Chauhan, S., Kossatz, U., Grunwald, V., Kubicka, S., Pich, A., Manns, M.P., *et al.* (2011). The SCF-FBXW5 E3-ubiquitin ligase is regulated by PLK4 and targets HsSAS-6 to control centrosome duplication. Nat Cell Biol *13*, 1004-1009.

Rieder, C.L., Faruki, S., and Khodjakov, A. (2001). The centrosome in vertebrates: more than a microtubule-organizing center. Trends Cell Biol *11*, 413-419.

Robbins, E., Jentzsch, G., and Micali, A. (1968). The centriole cycle in synchronized HeLa cells. J Cell Biol *36*, 329-339.

Rodrigues-Martins, A., Bettencourt-Dias, M., Riparbelli, M., Ferreira, C., Ferreira, I., Callaini, G., and Glover, D.M. (2007). DSAS-6 organizes a tube-like centriole precursor, and its absence suggests modularity in centriole assembly. Curr Biol *17*, 1465-1472.

Rogers, G.C., Rusan, N.M., Roberts, D.M., Peifer, M., and Rogers, S.L. (2009). The SCF Slimb ubiquitin ligase regulates Plk4/Sak levels to block centriole reduplication. J Cell Biol *184*, 225-239.

Roque, H., Wainman, A., Richens, J., Kozyrska, K., Franz, A., and Raff, J.W. (2012). Drosophila Cep135/Bld10 maintains proper centriole structure but is dispensable for cartwheel formation. J Cell Sci *125*, 5881-5886.

Schmidt, T.I., Kleylein-Sohn, J., Westendorf, J., Le Clech, M., Lavoie, S.B., Stierhof, Y.D., and Nigg, E.A. (2009). Control of centriole length by CPAP and CP110. Curr Biol *19*, 1005-1011.

Shinohara, H., Sakayori, N., Takahashi, M., and Osumi, N. (2013). Ninein is essential for the maintenance of the cortical progenitor character by anchoring the centrosome to microtubules. Biol Open *2*, 739-749.

Sonnen, K.F., Schermelleh, L., Leonhardt, H., and Nigg, E.A. (2012). 3D-structured illumination microscopy provides novel insight into architecture of human centrosomes. Biol Open *1*, 965-976.

Soung, N.K., Kang, Y.H., Kim, K., Kamijo, K., Yoon, H., Seong, Y.S., Kuo, Y.L., Miki, T., Kim, S.R., Kuriyama, R., *et al.* (2006). Requirement of hCenexin for proper mitotic functions of polo-like kinase 1 at the centrosomes. Mol Cell Biol *26*, 8316-8335.

Spektor, A., Tsang, W.Y., Khoo, D., and Dynlacht, B.D. (2007). Cep97 and CP110 suppress a cilia assembly program. Cell *130*, 678-690.

Tang, C.J., Fu, R.H., Wu, K.S., Hsu, W.B., and Tang, T.K. (2009). CPAP is a cell-cycle regulated protein that controls centriole length. Nat Cell Biol *11*, 825-831.

Thornton, G.K., and Woods, C.G. (2009). Primary microcephaly: do all roads lead to Rome? Trends In Genet *25*, 501-510.

Tsang, W.Y., Bossard, C., Khanna, H., Peranen, J., Swaroop, A., Malhotra, V., and Dynlacht, B.D. (2008). CP110 suppresses primary cilia formation through its interaction with CEP290, a protein deficient in human ciliary disease. Dev Cell *15*, 187-197.

Tsou, M.F., and Stearns, T. (2006). Controlling centrosome number: licenses and blocks. Curr Opin Cell Biol *18*, 74-78.

Tsou, M.F., Wang, W.J., George, K.A., Uryu, K., Stearns, T., and Jallepalli, P.V. (2009). Polo kinase and separase regulate the mitotic licensing of centriole duplication in human cells. Dev Cell *17*, 344-354.

Vassilev, L.T., Tovar, C., Chen, S., Knezevic, D., Zhao, X., Sun, H., Heimbrook, D.C., Chen, L. (2006). Selective small-molecule inhibitor reveals critical mitotic functions of human CDK1. Proc Natl Acad Sci U S A. *103*:10660–10665.

Van Breugel, M., Wilcken, R., McLaughlin, S.H., Rutherford, T.J., and Johnson, C.M. (2014). Structure of the SAS-6 cartwheel hub from Leishmania major. eLife *3*, e01812.
Vorobjev, I.A., and Chentsov Yu, S. (1982). Centrioles in the cell cycle. I. Epithelial cells. J Cell Biol *93*, 938-949.

Wang, X., Tsai, J.W., Imai, J.H., Lian, W.N., Vallee, R.B., and Shi, S.H. (2009). Asymmetric centrosome inheritance maintains neural progenitors in the neocortex. Nature *461*, 947-955.

Yamashita, Y.M., and Fuller, M.T. (2008). Asymmetric centrosome behavior and the mechanisms of stem cell division. J Cell Biol *180*, 261-266.

Zheng, X., Gooi, L.M., Wason, A., Gabriel, E., Mehrjardi, N.Z., Yang, Q., Zhang, X., Debec, A., Basiri, M.L., Avidor-Reiss, T., *et al.* (2014). Conserved TCP domain of Sas-4/CPAP is essential for pericentriolar material tethering during centrosome biogenesis. Proc Natl Acad Sci U S A *111*, E354-363.

# 국문초록

중심체는 한 쌍의 중심립과 이것을 둘러싸고 있는 PCM으로 이루어져 있다. 세포분열 과정에서 염색체와 마찬가지로 중심립은 복제가 되어 두 개의 딸세포로 나누어진다. 중심립은 한 번의 세포주기 동안 한 번만 복제가 일어나도록 엄격하게 조절이 된다. 이러한 조절이 제대로 일어나지 않으면 중심립/중심체의 개수에 이상이 생긴다. 중심체 개수의 이상은 염색체의 불안정성과 이로 인한 암의 형성과 관련이 깊다. 분열기에 중심체는 방추체로서의 기능을 수행하기 위하여 주변물질을 증가시키면서 PCM의 크기가 커진다. 이로 인해 강력한 미세소관을 형성할 능력을 가지게 된다. 이 과정을 중심체의 성숙과정이라고 한다. 만약, 중심체의 성숙과정이 일어나지 않으면, 염색체의 분리도 제대로 일어나지 않는다. 따라서, 세포주기 동안 중심체의 복제과정과 성숙과정을 규명하는 것은 중심체 연구에 있어서 아주 중요한 일이다. 이 논문에서는 중심체 복제과정과 성숙과정에 있어서 두 개의 중심체 단백질인 CPAP와 CP110의 기능을 연구하였다.

제 1장에서는, 중심체 성숙과정 동안 CPAP가 어떤 기능을 수행하는지 연구하였다. 기존의 연구에서 CPAP는 중심립의 형성과 길이신장에 필요하다고 알려져 있었다. 본 연구에서 CPAP가 중심체의 복제과정뿐만 아니라, 성숙과정에도 중요하다는 것을 밝혔다. 또한 CPAP의 중심체 성숙과정에서의 기능은 기존의 중심립 복제과정과는 독립적인 기능일 것으로 생각된다. CPAP의 siRNA를 통한 발현억제는 중심립의 성숙과정의 방해와 더불어 결국에는 분열기에 비대칭적인 방추체가 형성되도록 한다.

제 2장에서는, 중심립의 복제과정 동안 CP110이 어떤 기능을 수

행하는지 연구하였다. PLK4는 중심립 형성에 있어서 필수적인 인산화 효소이지만, 직접적인 기질에 관해서는 잘 알려지지 않았다. 본 연구에서는 중심체 단백질인 CP110이 PLK4에 의해 인산화가 되는 기질임을 밝혔다. 또한, CP110의 serine 98 인산화가 중심체의 복제과정에 있어서 중요하다는 것을 확인하였다. 인산화 항체를 통해, 중심립이 생겨나는 위치에서 CP110이 PLK4에 의해 인산화가 된다는 것을 확인하였다. 이 결과를 바탕으로, PLK4에 의한 CP110의 인산화가 중심립 형성인자들을 안정화 시킴으로서 중심체 복제과정에 관여하는 중요한 요소로 생각된다.

**주요어** : 중심체, CPAP, 중심체주변물질 (PCM), 중심체 성숙, CP110, PLK4, 중심체 복제

**학번** : 2010-30100